Bioactive Materials 41 (2024) 239–256

Contents lists available at ScienceDirect

Bioactive Materials

journal homepage: www.keaipublishing.com/en/journals/bioactive-materials

A five-in-one novel MOF-modified injectable hydrogel with thermo-sensitive and adhesive properties for promoting alveolar bone repair in periodontitis: Antibacterial, hemostasis, immune reprogramming, pro-osteo-/angiogenesis and recruitment

Shiyuan Yang [a,b,1], Yan Zhu [a,b,1], Chunxiao Ji [b,c], Huimin Zhu [a,b], An Lao [b,c], Ran Zhao [b,d], Yue Hu [a,b], Yuning Zhou [a,b], Jia Zhou [a,b], Kaili Lin [b,c,**], Yuanjin Xu [a,b,*]

[a] Department of Oral Surgery, Shanghai Ninth People's Hospital, Shanghai Jiao Tong University School of Medicine, Shanghai, China
[b] College of Stomatology, Shanghai Jiao Tong University, National Center for Stomatology, National Clinical Research Center for Oral Diseases, Shanghai Key Laboratory of Stomatology, Shanghai Research Institute of Stomatology, Shanghai, China
[c] Department of Oral and Cranio-maxillofacial Surgery, Shanghai Ninth People's Hospital, Shanghai Jiao Tong University School of Medicine, Shanghai, China
[d] Department of Oral Mucosal Diseases, Shanghai Ninth People's Hospital, Shanghai Jiao Tong University School of Medicine, Shanghai, China

ARTICLE INFO

Keywords:
Hydrogel
Periodontitis
Alveolar bone regeneration
Quercetin
ZIF-8

ABSTRACT

Periodontitis is a chronic inflammatory disease caused by plaque that destroys the alveolar bone tissues, resulting in tooth loss. Poor eradication of pathogenic microorganisms, persistent malignant inflammation and impaired osteo-/angiogenesis are currently the primary challenges to control disease progression and rebuild damaged alveolar bone. However, existing treatments for periodontitis fail to comprehensively address these issues. Herein, an injectable composite hydrogel (SFD/CS/ZIF-8@QCT) encapsulating quercetin-modified zeolitic imidazolate framework-8 (ZIF-8@QCT) is developed. This hydrogel possesses thermo-sensitive and adhesive properties, which can provide excellent flowability and post-injection stability, resist oral fluid washout as well as achieve effective tissue adhesion. Inspirationally, it is observed that SFD/CS/ZIF-8@QCT exhibits a rapid localized hemostatic effect following implantation, and then by virtue of the sustained release of zinc ions and quercetin exerts excellent collective functions including antibacterial, immunomodulation, pro-osteo-/angiogenesis and pro-recruitment, ultimately facilitating excellent alveolar bone regeneration. Notably, our study also demonstrates that the inhibition of osteo-/angiogenesis of PDLSCs under the periodontitis is due to the strong inhibition of energy metabolism as well as the powerful activation of oxidative stress and autophagy, whereas the synergistic effects of quercetin and zinc ions released by SFD/CS/ZIF-8@QCT are effective in reversing these biological processes. Overall, our study presents innovative insights into the advancement of biomaterials to regenerate alveolar bone in periodontitis.

1. Introduction

Periodontitis, as a chronic inflammatory disease caused by plaque microorganisms, can gradually destroy the periodontal support structures (especially the alveolar bone), eventually leading to tooth loss [1]. As one of the most common oral diseases worldwide, affecting 10–15 % of the global population [2]. For dentists, the recognized treatment strategy for periodontitis comprises three main and

Peer review under responsibility of KeAi Communications Co., Ltd.
* Corresponding author. Shanghai Ninth People's Hospital, Shanghai Jiao Tong University School of Medicine, 639 Zhizaoju Road, Shanghai, 200011, China.
** Corresponding author. Shanghai Ninth People's Hospital, Shanghai Jiao Tong University School of Medicine, 639 Zhizaoju Road, Shanghai, 200011, China.
E-mail addresses: yangshiyuan1996@sjtu.edu.cn (S. Yang), k.atherine@sjtu.edu.cn (Y. Zhu), chunxiaoxiaozi@163.com (C. Ji), zoehimi@126.com (H. Zhu), wzmulaoan@163.com (A. Lao), jjs3156@163.com (R. Zhao), moonhu1992@163.com (Y. Hu), xiaoyao7958@163.com (Y. Zhou), 18049963996@163.com (J. Zhou), linkaili@sjtu.edu.cn, lklecnu@aliyun.com (K. Lin), drxuyuanjin@126.com (Y. Xu).
[1] These authors contributed equally to this work.

https://doi.org/10.1016/j.bioactmat.2024.07.016
Received 8 November 2023; Received in revised form 7 July 2024; Accepted 13 July 2024

interconnected steps: antimicrobial therapy, inflammation control and periodontal regeneration [3]. Unfortunately, none of the existing clinical treatments is capable of completely addressing these issues [4]. Therefore, there is an urgent need to develop a new strategy for periodontitis to attain a comprehensive intervention.

In general, ideal periodontitis treatment, with the ultimate goal of alveolar bone regeneration and periodontal function restoration, is a highly organized biological process that relies on the interplay of multiple cells, molecules, and signaling pathways. As is well-known, *porphyromonas gingivalis* (*P. gingivalis*) plays a significant role in the periodontal microflora dysbiosis and local immune system imbalance, which can lead to decreased viability of endogenous mesenchymal stem cells (MSCs) and hyperinflammation of immune cells. Thus, inhibition of *P. gingivalis* infection is the primary goal in advancing periodontitis treatment and avoiding recurrence, which could effectively improve the deficient microenvironment at the site of periodontitis [5,6]. The dominant antimicrobial approaches involve systemic or topical application of antibiotics, which often have insufficient antimicrobial effectiveness or induce dysbiosis and drug-resistant strains, ultimately resulting in unsatisfactory therapeutic outcomes [7]. Therefore, there is an urgent need to discover a new antimicrobial strategy as an alternative to antibiotics. In addition, the amplified cascade of immune cells further aggravates the inflammatory response in periodontitis triggered by pathogenic bacteria, in which macrophages play a crucial role [8]. Macrophages as highly plastic immune cells are commonly classified into the pro-inflammatory M1 phenotype and the anti-inflammatory M2 phenotype [9]. In periodontitis, the M1 polarization of macrophages during the early inflammatory phase plays a critical role in tissue homeostasis and defense, whereas persistent maintenance of this state can worsen the periodontitis process and ultimately lead to irreversible destruction of periodontal tissues [10]. Reprogramming macrophages towards the M2 phenotype has been shown to effectively eliminate chronic inflammation and drive periodontal regeneration [11,12]. Hence, the promotion of macrophage phenotype switching from M1 to M2, while controlling bacterial infection, is essential to prevent the exacerbation of periodontitis and regenerate lost alveolar bone. Furthermore, increasing evidence suggested that the lack of endogenous PDLSCs in the area of bone defects and their impaired osteo-/angiogenic potential (caused by the dual persecution by *P. gingivalis* virulence factors and chronic inflammation) worsened the already challenging state of alveolar bone reconstruction in periodontitis [13,14]. Consequently, the successful recruitment and enhanced osteo-/angiogenesis of PDLSCs, based on overcoming the challenges of infection and immune, can effectively accelerate the healing process of alveolar bone defects caused by periodontitis. Furthermore, the enhancement of the angiogenic capacity of endothelial cells (a type of cell essential for angiogenesis) is believed to be pivotal for regenerating alveolar bone in the periodontitis microenvironment [15]. It is worth noting that the distinctive characteristics of the oral microenvironment permit the continued deposition of *P. gingivalis* on the teeth, thereby prolonging the periodontal disease process or causing recurrence [16]. Therefore, different from the general bone repair platform (only need antibacterial and immunomodulatory functions at the initial stage), the antibacterial and immunomodulatory functions of the treatment platform applied to alveolar bone defects under the periodontitis microenvironment may be required to carry through the entire tissue regeneration process, that is, a whole-course treatment platform (including antibacterial, immunomodulation, osteo-/angiogenesis and recruitment) is needed.

Thanks to significant advancements in tissue engineering, numerous biomaterials have been created to treat periodontitis, such as hydrogels, nanoparticles and electrospun membranes [17–21]. Among them, due to the characteristics of good fluidity during injection, fast sol-gel conversion after injection and strong adhesion to bone tissues, the injectable thermo-sensitive adhesive hydrogel is able to adapt to the irregular anatomical structure of periodontal pockets and resist the continuous flushing of gingival sulcus fluid, which attracted our attention to its potential application in managing alveolar bone defects in periodontitis [8,22]. In particular, incorporating bioactive nanoparticles into hydrogels has been recognized as an advantageous approach for promoting adaptation to specific periodontitis microenvironments [23]. Zeolitic imidazolate framework-8 (ZIF-8), a metal-organic framework (MOF) with excellent pH sensitivity, can intelligently respond to the periodontitis microenvironment to continuously release Zn^{2+}, facilitating critical antimicrobial, recruitment and osteo-/angiogenic processes [24,25]. Unfortunately, this bioactive nanoparticle lacks robust immunomodulatory property, thus limiting its utility in treating periodontitis [26]. Quercetin, a natural flavonoid known for its pharmacological effects such as antimicrobial, immunomodulatory, pro-migratory and pro-osteo-/angiogenic properties, has garnered considerable attention in recent years in the field of periodontitis treatment [27–30]. Inspired by the above theories, we proposed a quercetin-modified ZIF-8 nanoparticle (ZIF-8@QCT) based on the advantages of ZIF-8 while enhancing its immunomodulatory capacity, and then doped this nanoparticle into the injectable thermo-sensitive adhesive hydrogel to make it more suitable for regenerating alveolar bone under periodontitis.

Clinically, biomaterials are primarily used for alveolar bone regeneration via surgical implantation. Nevertheless, periodontal regeneration surgery is usually accompanied by heavy bleeding due to the abundance of blood vessels in the periodontal tissues, which can impede the surgery and lead to serious postoperative complications, so the rapid hemostatic property of biomaterials after implantation can greatly increase the success rate of the surgery.

Here, we mixed dopamine-modified silk fibroin (SFD) with the classic thermo-sensitive hydrogel (chitosan (CS)/β-glycerophosphate (β-GP)) and then crosslinked them using genipin to create an injectable dual-crosslinked hydrogel (SFD/CS) with thermo-sensitive and adhesive properties. Additionally, ZIF-8@QCT with pH-responsive property was doped into the hydrogel for the dual delivery of quercetin and zinc ions. Our experimental data supported that this composite hydrogel could exert rapid hemostasis after implantation, and then by playing collective functions (the effective reduction of *P. gingivalis*, the reprogramming of macrophages towards M2 polarization, the enhancement of osteo-/angiogenic property, and the acceleration of endogenous PDLSCs homing) eventually facilitated alveolar bone regeneration in periodontitis. RNA sequencing (RNA-seq) analysis further revealed that SFD/CS/ZIF-8@QCT could effectively address the issues of decreased energy metabolism, excessive oxidative stress, and over-activated autophagy caused by Pg. LPS via activating the PI3K-Akt signaling pathway, thus exhibiting excellent osteo-/angiogenic property of PDLSCs. Taken together, the present study not only revealed that SFD/CS/ZIF-8@QCT could promote alveolar bone regeneration by comprehensively addressing the various difficulties in periodontitis, but also disclosed the underlying mechanisms (energy metabolism, oxidative stress and autophagy) by which it promotes osteo-/angiogenesis of PDLSCs, thus providing promising avenues for future periodontitis management (see Scheme 1).

2. Results and discussion

2.1. Fabrication and characterization of ZIF-8 and ZIF-8@QCT

Both ZIF-8 and ZIF-8@QCT nanoparticles were prepared by the one-pot method previously reported in the literature [26]. Fig. 1A illustrated the detailed process for preparing nanoparticles. To the unaided eye, the dispersion of ZIF-8 nanoparticles appeared milky white, while the dispersion of ZIF-8@QCT nanoparticles had a ginger yellow hue (Fig. 1B). Transmission electron microscopy (TEM) revealed that both ZIF-8 and ZIF-8@QCT nanoparticles exhibited uniform dodecahedral morphology, while the diameter of ZIF-8@QCT was slightly larger than that of ZIF-8 (the particle size of ZIF-8 about 80~100 nm, the particle size of ZIF-8@QCT about 100~120 nm) (Fig. 1C; Figure S1, Supporting Information). Since both ZIF and ZIF-8@QCT were MOFs created through the coordination of Zn^{2+} and 2-methylimidazole (2-mIM), we

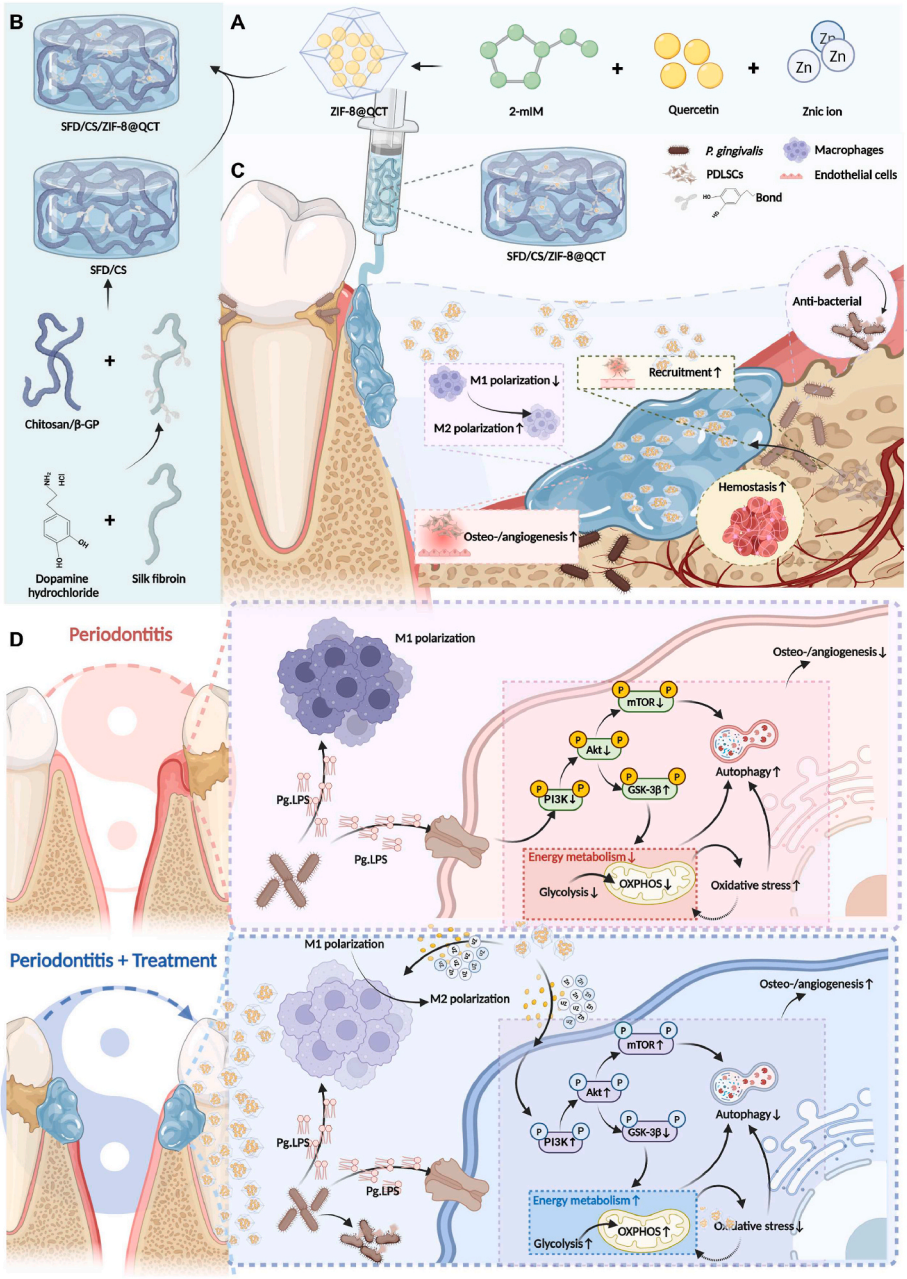

Scheme 1. Schematic illustration of the SFD/CS/ZIF-8@QCT composite hydrogel for regenerating alveolar bone in periodontitis. A) The preparation of ZIF-8@QCT. B) The preparation of SFD/CS/ZIF-8@QCT composite hydrogel. C) The SFD/CS/ZIF-8@QCT composite hydrogel promoted alveolar bone regeneration in periodontitis via antibacterial, hemostasis, immunoregulation, pro-osteo-/angiogenesis and pro-recruitment. D) The SFD/CS/ZIF-8@QCT composite hydrogel strengthened osteo-/angiogenesis of PDLSCs in periodontitis due to the strong promotion of energy metabolism as well as the powerful inhibition of oxidative stress and autophagy.

confirmed the homogeneous distribution of the zinc element using energy-dispersive X-ray (EDX) elemental mapping for both of the aforementioned nanoparticles (Figure S2, Supporting Information). The zeta potential assay demonstrated a reduction in zeta potential from ~+1.167 mV to ~ -1.660 mV following encapsulation of quercetin within ZIF-8, attributable to the negative potential of quercetin (Fig. 1D). The literature indicated that negative potential biomaterials had a superior capacity to stimulate osteogenic differentiation compared to positive potential biomaterials, within absolute values of 0~35 mV [31]. Besides, it has been reported that anionic nanoparticles were not only less susceptible to protein corona formation (which was more readily taken up by cells than cationic nanoparticles), but also promoted macrophage polarization towards M2 phenotype [32,33]. Subsequently, ultraviolet–visible (UV–Vis) spectrophotometry was employed to quantify the loading of quercetin, as shown in Fig. 1E. The acid-treated ZIF-8 solution did not exhibit any absorption peaks, but the acid-treated ZIF-8@QCT solution displayed notable peaks at ~420 nm, indicating successful encapsulation of quercetin within ZIF-8 nanoparticles, while the quercetin solution typically exhibited an absorption peak at a wavelength of ~374 nm (Fig. 1E). However, in the current study, the shift in the absorption spectrum of ZIF-8@QCT to ~420 nm could be attributed to the interaction between quercetin and zinc ions that decreased the band gap between the π-π electronic transitions of quercetin [34]. Moreover, according to the prepared quercetin standard curve, the drug loading of quercetin in ZIF-8@QCT was determined to be 13.51 % (Figure S3, Supporting Information). The X-ray diffraction

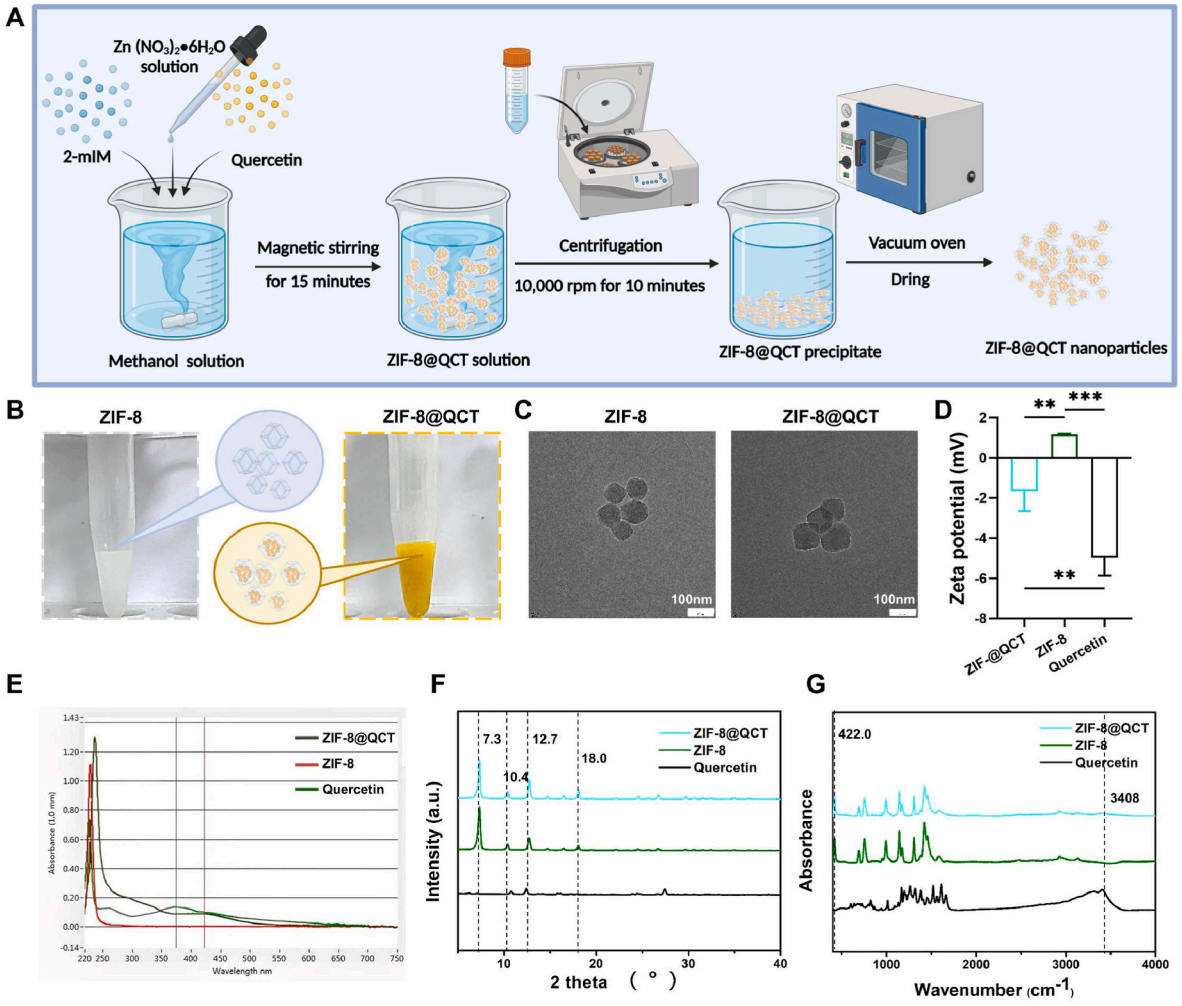

Fig. 1. Fabrication and characterization of ZIF-8 and ZIF-8@QCT. A) Synthesis procedure of ZIF-8@QCT. B) Images of ZIF-8 and ZIF-8@QCT solution. C) TEM images of ZIF-8 and ZIF-8@QCT nanoparticles. D) Zeta potential of ZIF-8 and ZIF-8@QCT nanoparticles as well as quercetin. E) UV–Vis spectra of acid treated ZIF-8 and ZIF-8@QCT solution as well as quercetin. F, G) XRD and FITR spectra of ZIF-8 and ZIF-8@QCT nanoparticles. Data are presented as mean ± SD. *P < 0.05, **P < 0.01, and ***P < 0.001.

(XRD) analysis revealed that both ZIF-8 and ZIF-8@QCT exhibited the typical ZIF-8 structure with high crystallinity, as evidenced by the diffraction peaks observed at 7.3°, 10.4°, 12.7°, and 18.0° in Fig. 1F. In particular, there was no significant difference in the crystal structures between ZIF-8 and ZIF-8@QCT, suggesting that quercetin was encapsulated within ZIF-8 and thus its diffraction peaks were masked. The fourier transform infrared spectroscopy (FTIR) patterns slightly indicated that the primary peak of absorption for ZIF-8@QCT was a combination of quercetin and ZIF-8 (Fig. 1G). Taken together, we confirmed the successful synthesis of ZIF-8 and ZIF-8@QCT nanoparticles.

2.2. Characterization of the composite hydrogels

First, we evaluate the thermo-sensitive behavior of hydrogels through the vial inversion method [35]. As indicated in Fig. 2A, SFD/CS, SFD/CS/ZIF-8, and SFD/CS/ZIF-8@QCT demonstrated free-flowing characteristics at 4 °C and quickly (~2 min) transformed into hydrogels at 37 °C, indicating their thermo-responsive gelation properties. The gelation time of our composite hydrogels was found to be significantly faster than that of general CS/β-GP thermo-sensitive hydrogels. In addition to the thermo-sensitivity brought about by CS/β-GP itself, the adhesive property of the SFD (the addition of which somewhat attenuated the fluidity of the CS/β-GP hydrogel) also played an important role in this. In addition, the cross-linking function of genipin is carried out by reacting with the primary amine bonds on CS and SFD, resulting in the formation of a stable blue pigment [36]. Consequently, the cross-linking of the prepared composite hydrogels could be evaluated by observing its color. Therefore, it could be observed thar these hydrogels could be almost completely crosslinked via the action of genipin after 24 h to form dual-crosslinked network (Figure S4, Supporting Information). Such dual-crosslinked network enhanced mechanical strength and made them more suitable for restoring periodontal bone defects [37]. In Fig. 2B, we displayed the precise two-step transformation mechanism of the process outlined in Fig. 2A: (1) From 4 °C to 37 °C: as the temperature rose, the electrostatic attraction between CS and β-GP was destroyed, causing the dehydration of the CS chain and the replacement of water molecules with glycerol molecules, which leaded to the formation of a large number of hydrogen bonds between the CS chains and then resulted in gelation; (2) After 24 h at 37 °C: the free amino groups of SFD and CS underwent covalent dual-crosslinking in the presence of genipin [38,39]. As shown in Fig. 2C, the composite hydrogels we developed displayed excellent injectability both in air and under water, indicating their suitability for syringe injections into periodontitis bone defects which were damp and intricately shaped [23]. The scanning electron microscopy (SEM) images presented in Fig. 2D indicated that all composite hydrogels displayed irregular porous networks. Upon assessing the pore size and the porosity of each hydrogel group utilizing the SEM images, it was discovered that the SFD/CS group exhibited the

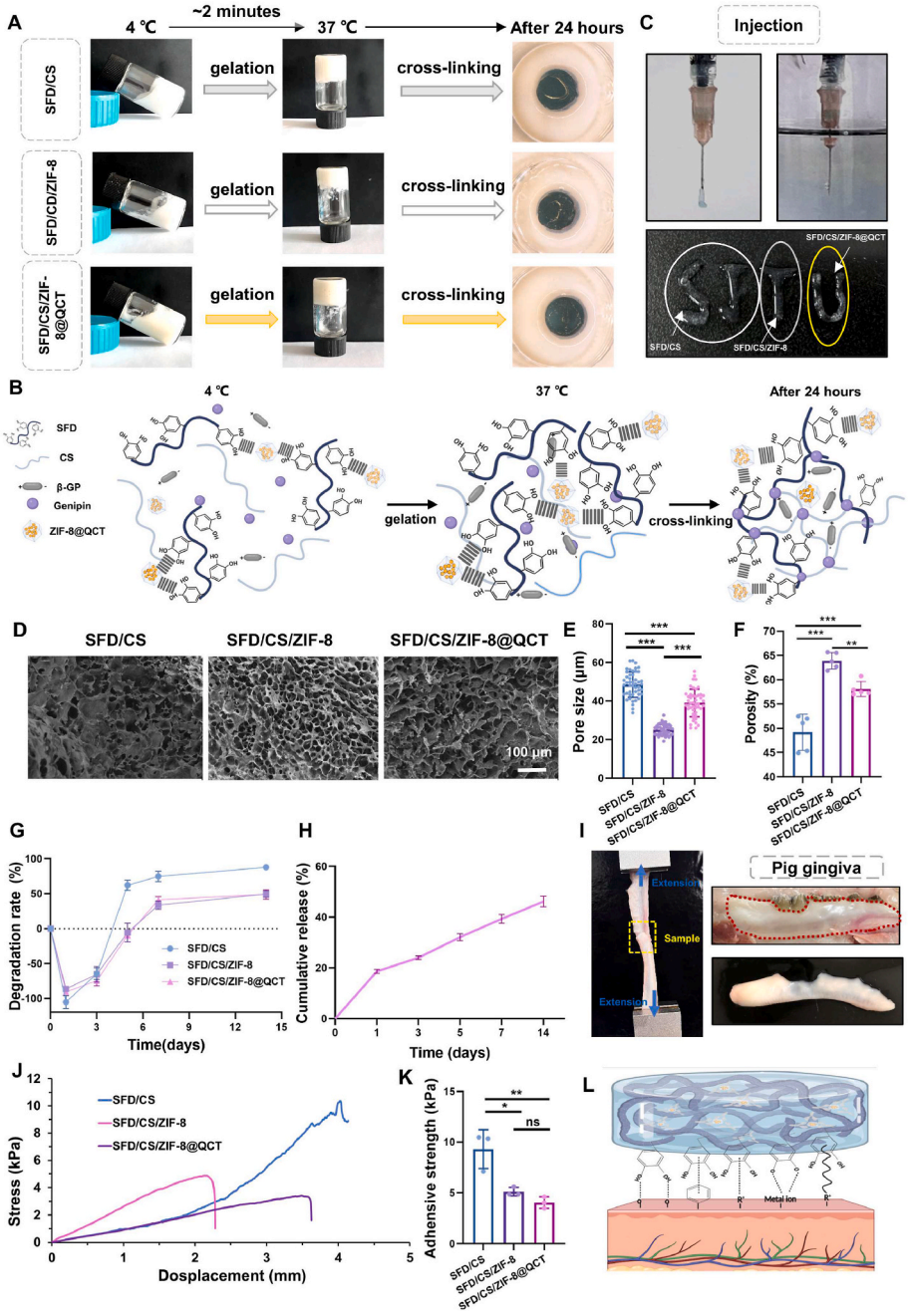

Fig. 2. Characterization of composite hydrogels. A) Optical photographs of SFD/CS, SFD/CS/ZIF-8 and SFD/CS/ZIF-8@QCT at 4 °C and 37 °C as well as after gelation for 24 h. B) Illustration of intra- and intermolecular interactions as described by the process in (A) using SFD/CS/ZIF-8 as an example. C) The injectability of SFD/CS, SFD/CS/ZIF-8 and SFD/CS/ZIF-8@QCT in air and under water. D-F) Representative SEM images as well as the quantification of pore size and porosity of the lyophilized composite hydrogels after gelation for 24 h. G) The degradation rate of the composite hydrogels. H) The cumulative release of QCT from SFD/CS/ZIF-8@QCT. I) Representative optical photographs of the lap-shear adhesive strength test using pig gingiva. J, K) The stress-strain curve and adhesion strength of the composite hydrogels. L) The adhesion mechanism of catechol groups by interacting with the substrate via hydrogen bonding, π-π interaction, cation-π bonding, coordination bonding, or covalent linking (from left to right). Data are presented as mean ± SD. *P < 0.05, **P < 0.01, and ***P < 0.001; ns, not significant.

largest pore size (about 50 μm), succeeded by the SFD/CS/ZIF-8@QCT group (about 40 μm), and finally the SFD/CS/ZIF-8 group (about 30 μm), while the ranking of porosity among the three groups (SFD/CS/ZIF-8 about 60~65 %, SFD/CS/ZIF-8@QCT about 55~60 % and SFD/CS about 45~50 %) was opposite (Fig. 2E–F). These findings could potentially be elucidated by the chelation of zinc ions with the catechol groups present in SFD. The weaker chelation effect of ZIF-8@QCT, as compared to ZIF-8, might be a result of certain zinc ions binding to the catechol bond in quercetin and consequently reducing the number of available zinc electron sites [40]. The EDX results showed even distribution of zinc element in the porous network structure of SFD/CS/ZIF-8 and SFD/CS/ZIF-8@QCT, confirming the successful doping of ZIF-8 and ZIF-8@QCT nanoparticles in the hydrogels (Figure S5, Supporting Information). In addition, we found that the addition of ZIF-8 and ZIF-8@QCT had a minor impact on swelling ratio of the SFD/CS hydrogel, causing a slight decrease but still maintaining the ratio higher than 80 %. Meanwhile, no significant difference was observed between the SFD/CS/ZIF-8 and SFD/CS/ZIF-8@QCT groups (Figure S6, Supporting Information). Taken together, the addition of nanoparticles increased the porosity of the hydrogel while maintaining

its high swelling ratio, which facilitated nutrient entry and metabolite efflux, osteoblast and blood vessel growth [41].

To date, several studies have emphasized the significance of a suitable degradation rate of hydrogels for bone regeneration [42,43].To assess the *in vitro* degradation rate, 100 μL of the composite hydrogels were incubated in 1 mL of artificial saliva at 37 °C (Fig. 2G). The results showed that the hydrogels of each group reached the swelling equilibrium at 24 h. Subsequently, the composite hydrogels degraded gradually over time, and there was no significant difference in the degradation rate among the three groups between 1 to 3 days. However, the degradation rate of SFD/CS was considerably faster than that of the nanoparticle-decorated hydrogels at later stages. By the 14th day, the SFD/CS group had only retained 10 % of their initial weight, whereas the SFD/CS/ZIF-8 and SFD/CS/ZIF-8@QCT groups still maintained 50 % of their original weight. It could be concluded that all of our prepared hydrogels displayed excellent biodegradability. And the incorporation of nanoparticles extended the degradation rate of the composite hydrogels, making them more aligned with the rate of bone regeneration, probably due to the robust interaction between zinc ions in the MOFs and the hydrogel network (i.e., zinc ions in ZIF-8 or ZIF-8@QCT nanoparticles interacted with catechol groups in SFD) [44]. In addition, we also evaluated the quercetin release profile in the SFD/CS/ZIF-8@QCT composite hydrogel and observed a gradual release pattern of quercetin that was consistent with the hydrogel's degradation

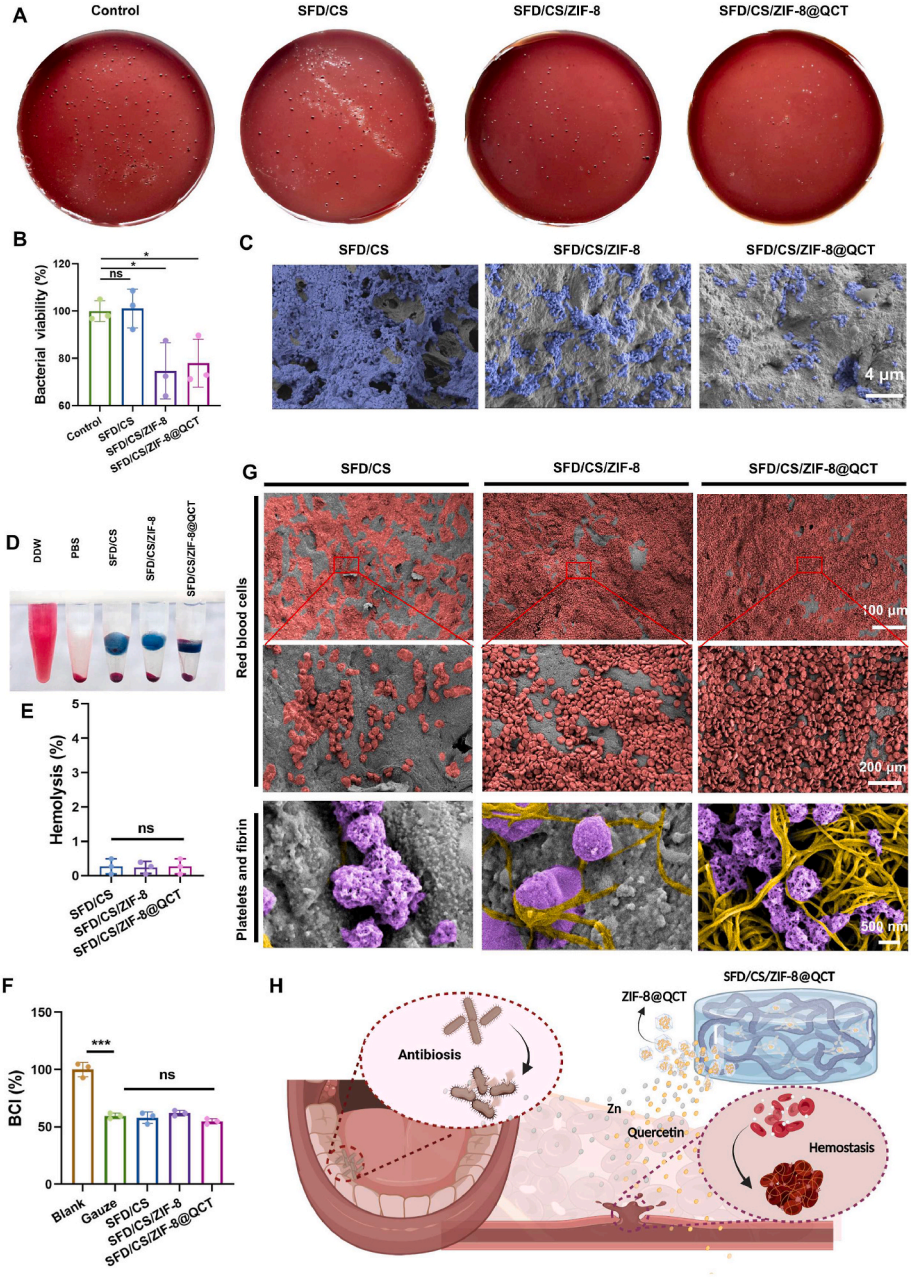

Fig. 3. Antibacterial and hemostatic properties of composite hydrogels. A) Optical photographs of the *P. gingivalis* colonies on blood agar plates treated by SFD/CS, SFD/CS/ZIF-8 and SFD/CS/ZIF-8@QCT on 12 h. B) Bacterial viability of *P. gingivalis* treated by SFD/CS, SFD/CS/ZIF-8 and SFD/CS/ZIF-8@QCT on 24 h. C) Representative SEM images of *P. gingivalis* treated by SFD/CS, SFD/CS/ZIF-8 and SFD/CS/ZIF-8@QCT on 48 h. D, E) Hemolytic representative optical images and its quantification of SFD/CS, SFD/CS/ZIF-8 and SFD/CS/ZIF-8@QCT. F) BCI value of SFD/CS, SFD/CS/ZIF-8 and SFD/CS/ZIF-8@QCT. G) Representative SEM images of erythrocytes, platelets and fibrin adhesion on the surface of the SFD/CS, SFD/CS/ZIF-8 and SFD/CS/ZIF-8@QCT. H) Schematic illustration describing the antibacterial and hemostatic properties of SFD/CS/ZIF-8@QCT. Data are presented as mean ± SD. *P < 0.05, **P < 0.01, and ***P < 0.001; ns, not significant.

rate (Fig. 2H). The sustained release of quercetin ensured its capability to consistently produce pharmacological activity, targeting bone defects in periodontitis and thereby assisting in the treatment of such disease.

In addition to the aforementioned properties, the ideal biomaterials for regenerating the damaged alveolar bone in periodontitis are expected to have the property of adhering to the surface of the periodontal tissue to resist the continuous flushing of gingival sulcus fluid and remain in the periodontal pockets for an extended period of time, thus enabling a gradual and steady release of the drug [45]. As shown in Figure S7 (Supporting Information), the SFD/CS composite hydrogel displayed exceptional adhesion on rubber, plastic, and metal (in air and under water) surfaces, thanks to the catechol groups in the SFD chain. To further assess the tissue adhesion of the composite hydrogels, a standard *in vitro* lap-shear test was performed using porcine gingiva (Fig. 2I). The study results indicated that the SFD/CS had an average adhesion strength of about 9.3 kPa, whereas the composite hydrogels' adhesion strength decreased to around 5.1 kPa and 4.0 kPa upon adding ZIF-8 and ZIF-8@QCT nanoparticles, respectively (Fig. 2J–K). The decrease of adhesion strength in composite hydrogels modified with MOFs can be attributed to the metal coordination reaction between the zinc ions in the MOFs and the catechol groups in the long chain of the SFD, which occupy the interfacial interaction site [46]. Fig. 2L demonstrated the specific adhesion mechanism of the composite hydrogel utilizing the catechol groups in the SFD, which interacted with tissue through a variety of bonding mechanisms including hydrogen bonding, π-π interaction, cation-π bonding, coordination bonding, or covalent linking [40].

2.3. Antibacterial property of composite hydrogels

Plaque is acknowledged as the initiator of periodontitis, in which *P. gingivalis* has been identified by researchers as the significant causal factor in the disease's progression. *P. gingivalis* releases a broad spectrum of virulence factors that trigger inflammation and subsequently cause tissue destruction [47]. Given the distinctive role of bacteria in periodontitis, it is imperative for biomaterials utilized in the treatment of this ailment to exhibit strong antimicrobial properties. To assess the antibacterial effect of the composite hydrogels on *P. gingivalis*, we incubated the hydrogels with *P. gingivalis*. The data presented in Fig. 3A demonstrated a decrease in the number of colonies on blood agar plates in all hydrogel-treated groups when compared with the control group. Additionally, the reduction in the SFD/CS/ZIF-8@QCT group was more notable than that observed in the SFD/CS/ZIF-8 group when compared to the SFD/CS group. Fig. 3B displayed the bacterial viability after 24 h of incubation, indicating no considerable variance between the control and SFD/CS groups. This result may be attributed to the high initial bacterial population, the feeblish antibacterial effect of the SFD/CS group and the presence of dead bacteria in the medium, resulting in no significant difference in absorbance between the control and SFD/CS groups. And on top of that, a statistically significant decrease was observed in both the SFD/CS/ZIF-8 and SFD/CS/ZIF-8@QCT groups when compared to the control and SFD/CS groups, with no significant differences between the groups. Furthermore, we utilized SEM to observe the bacteria on the hydrogel surface after 48 h of co-culture. The results showed that *P. gingivalis* adhered densely to the surface of the SFD/CS hydrogel, whereas the number of bacteria attached to the SFD/CS/ZIF-8 and SFD/CS/ZIF-8@QCT groups was significantly reduced, especially in the latter group (Fig. 3C). Taken together, SFD/CS/ZIF-8@QCT displayed robust antimicrobial qualities, potentially attributed to the synergistic release of zinc ions and quercetin.

CS, a natural polysaccharide with positive charges, exhibits antimicrobial effects through interfering with cell walls, interacting with bacterial DNA, and chelating bacterial nutrients [48]. Depending on the low concentration of CS added, our basal hydrogel SFD/CS exhibited some degree of antimicrobial property. As a MOF containing zinc, ZIF-8 can exert antibacterial effect by releasing zinc ions, whose antibacterial mechanism is mainly achieved through the destruction of cell membranes, DNA and proteins [49]. Quercetin, as a natural flavonoid, has been shown to exert antimicrobial effects by inhibiting gingipain activity, hemolytic activity, hemagglutination activity, biofilm formation, aggregation, and virulence gene expression in *P. gingivalis* [29]. ZIF-8@QCT, a quercetin-decorated ZIF-8, can be loaded onto SFD/CS composite hydrogels to synergistically release zinc ions and quercetin, thereby enhancing the already pre-existing antimicrobial effect of CS and demonstrating superior antimicrobial potential over the addition of ZIF-8.

2.4. Hemostatic properties of composite hydrogels

To our knowledge, previous studies have not taken into account the exceptional hemostatic properties when designing hydrogels to treat alveolar bone defects in periodontitis. During clinical application, regenerative periodontal surgery is necessary to implant biomaterials into the periodontal defect area for the alveolar bone regeneration. In addition to the bleeding that the surgery itself will surely cause, the characteristic of fragile and easy-to-bleed periodontal soft tissues under periodontitis will lead to excessive localized bleeding that is not conducive to injury management [50]. Therefore, we believe that the optimal biomaterials for alveolar bone regeneration in periodontitis should ideally have rapid hemostatic properties to optimize clinical application and facilitate wound care. Herein, we comprehensively evaluated the hemostatic properties of the composite hydrogels by investigating their hemolytic properties, blood coagulation index (BCI), aggregation capacity for erythrocytes and platelets as well as *in vivo* hemostatic capacity. As depicted in Fig. 3D–E, the composite hydrogels including SFD/CS, SFD/CS/ZIF-8, and SFD/CS/ZIF-8@QCT demonstrated no considerable hemolysis, while their hemolysis ratio was all less than 1 %, indicating excellent blood compatibility [23]. Moreover, BCI experiments were conducted and it was understanded that, as indicated by previous studies, decreased BCI values corresponded with enhanced hemostatic performance *in vitro* [51]. The results demonstrate that the BCI value of the gauze and composite hydrogel groups was significantly lower than that of the blank group, but the difference between these groups was not significant, indicating that the composite hydrogels we prepared all exhibited excellent hemostatic performance as gauze (Fig. 3F; Figure S8, Supporting Information). Subsequently, given that the aggregation of red blood cells, platelets and fibrin facilitates effective wound sealing, we observed the adhesion and aggregation of these elements on each composite hydrogel group to further analyze its hemostatic mechanisms [52]. SEM images showed that all hydrogel surfaces presented irregular erythrocyte aggregation, while SFD/CS group showed the least erythrocyte adhesion, followed by the SFD/CS/ZIF-8 group, and lastly the SFD/CS/ZIF-8@QCT group. Furthermore, platelets adhered to all hydrogels, while SFD/CS/ZIF-8 and SFD/CS/ZIF-8@QCT surfaces exhibited notable fibrin adhesion. Among them, platelets and fibrin were more abundant on the surface of the SFD/CS/ZIF-8@QCT group than on the surface of the SFD/CS/ZIF-8 group, which intermingled to form a high-density network in the former group (Fig. 3G).

Rodent tail and liver bleeding models were established to further evaluate the *in vivo* hemostatic ability of composite hydrogels, while the experimental procedure was shown in Figure S9A and S9D (Supporting Information). The results of tail amputation model showed that blood loss was significantly lower in all composite hydrogel groups than in the blank group. In particular, when applied to the tail bleeding site, the three composite hydrogels quickly stopped the bleeding. The MOFs-modified composite hydrogels exhibited lower blood loss than the SFD/CS hydrogel, with no significant difference observed between the SFD/CS/ZIF-8 and SFD/CS/ZIF-8@QCT composite hydrogels (Figure S9B-C, Supporting Information). Furthermore, the outcomes of the liver hemorrhage model yield strong evidence supporting the swift hemostatic capacity of our composite hydrogels, despite the absence of noteworthy distinctions among the three composite hydrogels

(Figure S9E-F, Supporting Information). These results indicated that all of our prepared composite hydrogels had a rapid and efficient hemostatic effect at first few minutes after implantation, and the addition of MOFs could enhance this effect to some degree.

Overall, our study demonstrated that the doping of ZIF-8@QCT could enhance the aggregation of erythrocytes, platelets, and fibrin on the hydrogel surfaces as well as slightly improve the *in vivo* hemostatic properties while maintaining excellent blood compatibility and BCI, ultimately leading to improved hemostatic properties of SFD/CS. Such results might be attributed to the following mechanisms: (1) It has been reported that catechol groups could bind to cationic charges and immediately (<1s) form complexes intermolecularly with plasma proteins, thereby acting as a hemostatic barrier membrane [53]. The rapid hemostatic function of our composite hydrogels was primarily attributable to the catechol groups on the long chain of SFD. (2) The positively charged CS could capture negatively charged erythrocytes by electrostatic attraction assisted the rapid hemostatic function of SFD, which might explain the intrinsic reason for the hemostasis of the basal SFD/CS composite hydrogel [54]. (3) It has been shown in the literatures that zinc ions could enhance platelet aggregation and accelerate fibrin production, thereby shortening the clotting time and accelerating clot formation [55]. However, since ZIF-8@QCT was chelated by the catechol groups on the SFD in the composite hydrogels, the release of zinc ions was not rapid, but occurred mainly at the coagulation interface after the catechol groups had exerted its rapid coagulation effect. (4) ZIF-8@QCT exhibited weaker chelation of catechol groups on SFD in comparison to ZIF-8, as previously elucidated. It could be concluded that SFD/CS/ZIF-8@QCT had excellent antimicrobial and pro-hemostatic effects (Fig. 3H).

2.5. Immunomodulatory properties of composite hydrogels

Current researches indicated that *P. gingivalis* stimulated the accumulation of macrophages, which triggered an hyperinflammatory response leading to destruction of periodontal tissue. Simultaneously, decomposed periodontal tissues provided nutrients required for growth of periodontal pathogenic bacteria, creating a positive feedback loop that worsens periodontitis [12,56]. Inspired by this theory, it is also crucial to control the excessive inflammatory response of macrophages while eliminating *P. gingivalis*. Based on mechanism studies of macrophages in periodontitis, the early presence of M1 macrophages supports tissue defense and resistance to bacterial invasion, whereas persistent M1 activation leads to prolonged and exacerbated inflammation, ultimately resulting in malignant tissue destruction and impaired healing [57]. Reprogramming macrophages from the M1 phenotype into the M2 phenotype has shown promising outcomes in hastening the regression of inflammation and facilitating tissue regeneration [58–61]. Therefore, biomaterials which can reprogram macrophages towards M2 polarization are ideal for treating periodontitis.

In order to evaluate the immunomodulatory properties of composite hydrogels under the *in vitro* periodontitis microenvironment, bone marrow-derived macrophages (BMDM) were successfully isolated from mouse femurs. Given that *P. gingivalis*-derived lipopolysaccharide (Pg. LPS) represented a key virulence factor of *P. gingivalis*, we added Pg. LPS to the culture medium at a concentration of 1 μg/mL in order to mimic the *in vitro* periodontitis microenvironment and simulate macrophage polarization. Furthermore, the composite hydrogel was co-cultured with the BMDM in the form of transwell, i.e., the composite hydrogels were placed in the transwell chambers while the cells were inoculated in the lower chambers. Given that good cytocompatibility is an important requirement for the clinical application of biomaterials, we firstly used cell counting kit-8 (CCK-8) assay to investigate the effect of composite hydrogels on cell viability (Figure S10, Supporting Information). The results showed no noteworthy variations in cell viability across any of the groups, suggesting excellent cell compatibility for the Pg. LPS and the composite hydrogel groups. RT-qPCR experiments demonstrated that Pg. LPS significantly increased the expression of M1 marker genes (IL-6, iNOS and TNF-α), while inhibiting the expression of M2 marker genes (Arg-1, CD206 and TGF-β). These observations suggested that the immune microenvironment triggered by *P. gingivalis* in periodontitis predominantly polarized macrophages toward M1 and suppressed M2 polarization. Compared to the Pg. LPS group, the SFD/CS hydrogel showed the lowest inhibitory effect on M1polarization (inhibitory effect of the IL-6 and iNOS gene expression as well as no effect of the TNF-α gene expression) and the minimal promotive effect on M2 polarization (no effect of the Arg-1 and CD206 gene expression as well as slight promotive effect of the TGF-β gene expression) among the three hydrogel-treated groups. In addition, compared to the SFD/CS composite hydrogel, the SFD/CS/ZIF-8 composite hydrogel generated a greater inhibition of M1 markers, while better promoting the gene expression of M2 marker. It was noteworthy that the SFD/CS/ZIF-8@QCT group exhibited the most potent inhibition of IL-6 and TNF-α as well as promotion of all M2 markers at gene level, while the effect on the gene expression of iNOS was indistinguishable from this of the SFD/CS/ZIF-8 group (Fig. 4B–G). Thereafter, we conducted immunofluorescence staining and demonstrated that the ZIF-8@QCT-decorated composite hydrogel was the most potent in inhibiting the expression of M1 marker protein (IL-6 and iNOS) and increasing the expression of M2 marker protein (Arg-1 and CD206) under the periodontitis microenvironment, followed by the ZIF-8-decorated group, and then the SFD/CS group (which only exhibited anti-inflammatory function without pro-M2 polarization) (Fig. 4H–L). Taken together, the results indicated that the synergistic release of zinc ions and quercetin from SFD/CS/ZIF-8@QCT resulted in a more potent immune reprogramming function than SFD/CS/ZIF-8 alone, which could effectively drive the reprograming of macrophages from the M1 phenotype to the M2 phenotype.

The structure of catechol group has been demonstrated to possess anti-inflammatory and antioxidant properties [62]. Therefore, the anti-inflammatory activity of SFD/CS in this study might originate from the catechol groups in SFD. Zinc element is a crucial micronutrient for the development of the adaptive immune system, which has been demonstrated to possess anti-inflammatory properties by inhibiting macrophage M1 polarization [63]. Our research aligned with this by indicating that SFD/CS/ZIF-8 drove M1 polarization to some extent but weakly promoted M2 polarization. Compared to ZIF-8, ZIF-8@QCT released not only zinc ions, but also quercetin with anti-inflammatory and macrophage reprogramming functions [64]. In conclusion, the use of SFD/CS/ZIF-8@QCT shows promising potential for immune reprogramming in periodontitis.

2.6. Effect of composite hydrogels on osteo-/angiogenic differentiation of PDLSCs under periodontitis

Consistent with the above, we first cultured PDLSCs with composite hydrogels as well as conducted live/dead staining and CCK-8 assays to assess cytocompatibility. As shown in Fig. 5A, the live/dead staining assay demonstrated that the cells in all groups maintained nearly complete viability (green) after 1, 4, 7 days of culture, indicating the absence of cytotoxicity in any of the composite hydrogels. Furthermore, the CCK-8 assay provided additional quantification of the impact of composite hydrogels on cell viability. There were no notable statistical differences in cell viability between groups after 1 and 4 days of incubation. Additionally, no significant statistical variances were observed in cell viability between the control and Pg. LPS groups after 7 days of incubation, while the hydrogel-containing groups showed a slightly improved cell viability compared to the Pg. LPS group (Fig. 5B). In conclusion, our composite hydrogels have good safety for PDLSCs.

As promising oral MSCs that are capable of forming a range of periodontal tissues under suitable induction conditions, PDLSCs are deemed to hold tremendous potential for alveolar bone regeneration under periodontitis [65]. The local chronic inflammatory microenvironment of periodontitis inhibits the osteogenic ability of PDLSCs,

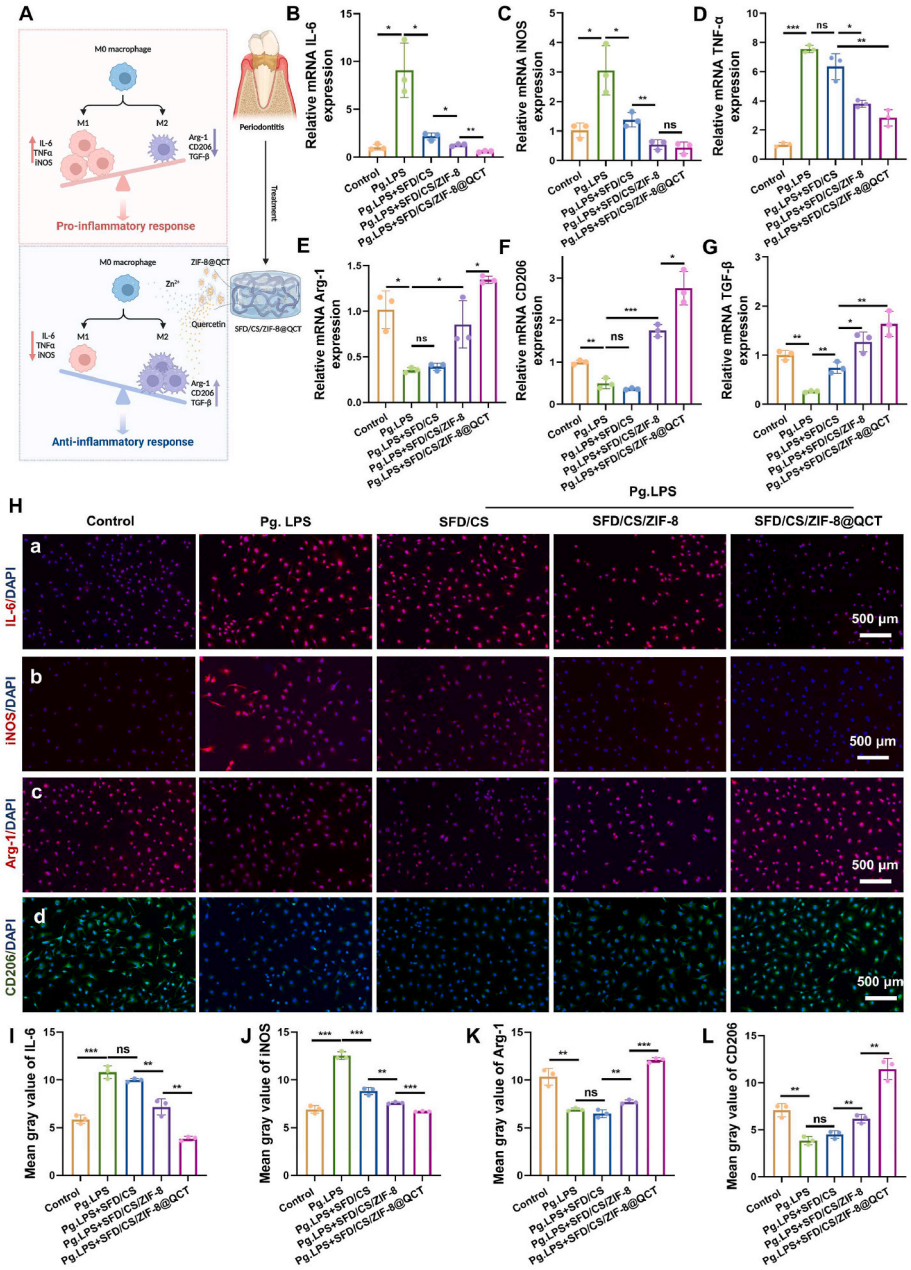

Fig. 4. Immunomodulatory properties of composite hydrogels. A) Schematic illustration depicting the macrophage reprogramming function of SFD/CS/ZIF8@QCT. B-G) Relative mRNA expression of M1-related genes (IL-6, TNF-α and iNOS) and M2-related genes (Arg-1, CD206 and TGF-β) of macrophages on day1 measured by RT-qPCR. H-L) The immunofluorescence staining and its quantitative analysis of M1-related protein (IL-6 and iNOS) and M2-related protein (Arg-1 and CD206) of macrophages on day1. Data are presented as mean ± SD. *P < 0.05, **P < 0.01, and ***P < 0.001; ns, not significant.

resulting in the inability to regenerate alveolar bone well [13]. Therefore, promoting the osteogenic differentiation of PDLSCs in the periodontitis microenvironment is of great significance to facilitate alveolar bone regeneration. Herein, we assessed the early and late pro-osteogenic impacts of composite hydrogels on PDLSCs in the periodontitis microenvironment utilizing Alkaline phosphatase (ALP) and Alizarin Red S (ARS) staining. The representative photographs of the ALP staining showed weaker staining in the Pg. LPS group compared with the control group after 7 days of culture, indicating that Pg. LPS inhibited the early osteogenic differentiation of PDLSCs, while the addition of SFD/CS did not significantly reverse this inhibitory effect. Additionally, both composite hydrogels modified with ZIF-8 and ZIF-8@QCT effectively reversed the suppressed intensity of ALP staining caused by the inflammatory microenvironment, with the latter showing superiority over the former (Fig. 5C; Figure S11, Supporting Information). During the late osteogenic induction stage, the ARS staining data demonstrated that the SFD/CS hydrogel significantly increased the number of calcium nodules impeded by Pg. LPS, while the results of the MOFs-modified composite hydrogel groups showed a similar trend to the ALP experiments (Fig. 5D; Figure S12, Supporting Information). Next, we utilized RT-qPCR and immunofluorescence staining assays to examine the impact of composite hydrogels on the osteogenic differentiation of PDLSCs at the gene and protein levels. As shown in the results of Fig. 5E–H, the addition of composite hydrogels significantly reversed the inhibitory effect of Pg.LPS on the expression of osteogenic genes (ALP, OCN, OPN, and OSX), with the strongest boosting effect of the composite hydrogel loaded with ZIF-8@QCT, followed by the composite hydrogel loaded with ZIF-8, and then again by the pure SFD/CS composite

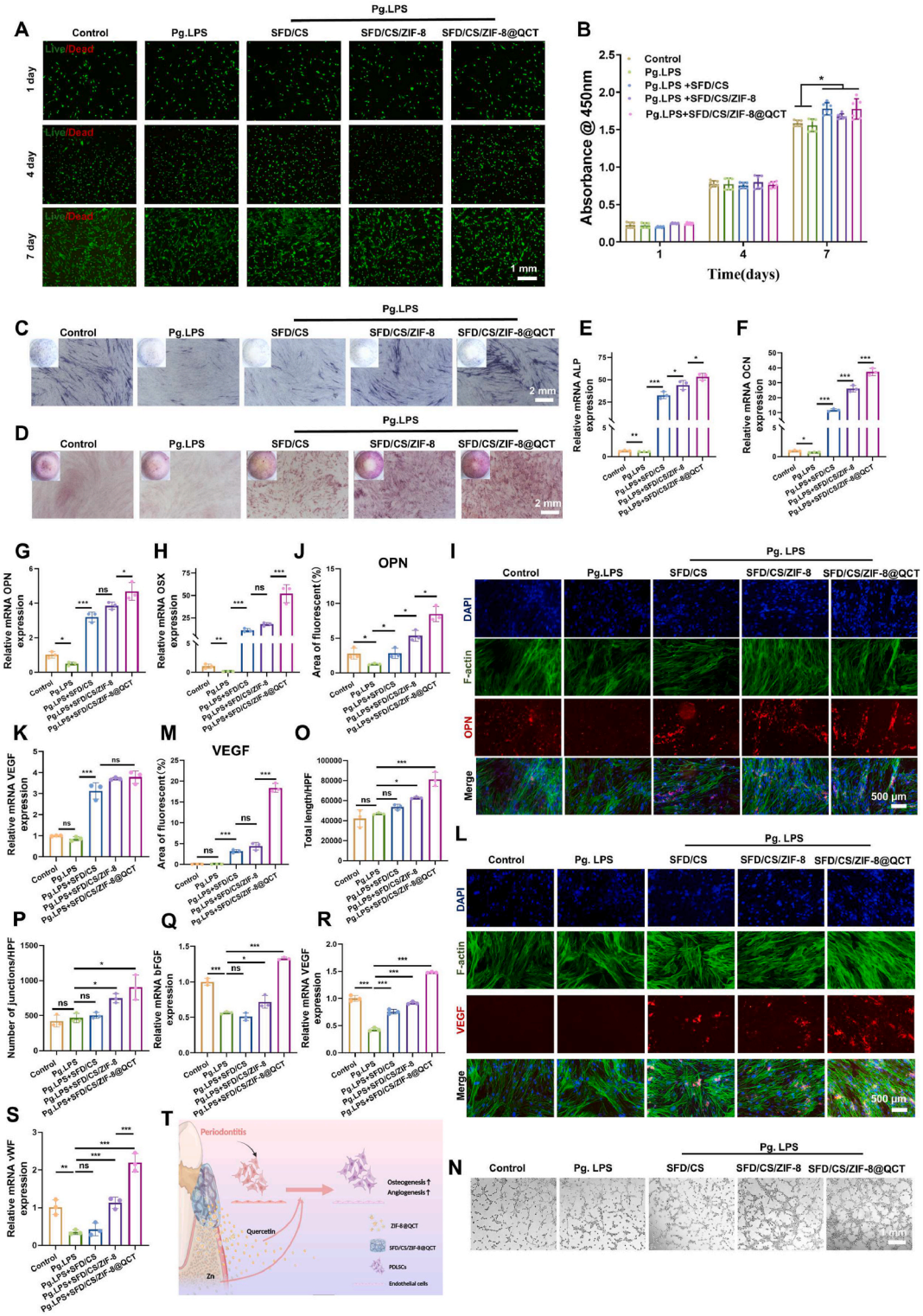

Fig. 5. Effect of composite hydrogels on osteo-/angiogenesis under periodontitis A) Representative fluorescence images of PDLSCs on day 1, 4, 7 evaluated using live/dead staining. B) Cell viability of PDLSCs on day 1, 4, 7 evaluated using CCK-8. C) Representative optical images of PDLSCs on day 7 evaluated using ALP staining. D) Representative optical images of PDLSCs on day 7 evaluated using ARS staining. E-H) Relative mRNA expression of osteogenesis-related genes (ALP, OCN, OPN and OSX) and angiogenesis-related gene (VEGF) of PDLSCs on day7 measured by RT-qPCR. I, J) The immunofluorescence staining and its quantitative analysis of osteogenesis-related protein (OPN) of macrophages on day7. K) Relative mRNA expression of angiogenesis-related gene (VEGF) of PDLSCs on day7 measured by RT-qPCR. L, M) The immunofluorescence staining and its quantitative analysis of angiogenesis-related protein (VEGF) of macrophages on day7. N–P) Tube formation of HUVECs stimulated for 3 days and its quantitative analysis of total length and number of junctions. Q-S) Relative mRNA expression of angiogenesis-related gene (bFGF, VEGF and vWF) of HUVECs stimulated for 3 days measured by RT-qPCR. T) Schematic illustration depicting the pro-osteo-/angiogenic function of SFD/CS/ZIF8@QCT. Data are presented as mean ± SD. *P < 0.05, **P < 0.01, and ***P < 0.001; ns, not significant.

hydrogel group. Immunofluorescence staining images further confirmed that Pg. LPS hindered the expression of OPN, while the SFD/CS/ZIF-8@QCT group showed the highest secretion of OPN protein among the three composite hydrogel groups consistent with RT-qPCR results (Fig. 5I–J). Summarizing these findings, we concluded that the periodontitis microenvironment impeded the osteogenic differentiation of PDLSCs, whereas the SFD/CS hydrogel could partially reverse this process, with a more pronounced effect observed at later stages. Inspiringly, the pro-osteogenic effect of ZIF-8 or ZIF-8@QCT-modified composite hydrogels was more exciting than that of SFD/CS, in which the SFD/CS/ZIF-8@QCT had a stronger effect than SFD/CS/ZIF-8 due to the dual pro-osteogenic effects of zinc ions and quercetin [66,67].

Bone tissue is highly vascularized, with interdependence between angiogenesis and osteogenesis [68]. Thus, enhancing the osteogenic differentiation of PDLSCs and the angiogenesis of endothelial cells are essential for optimal regeneration of periodontal bone tissue [69]. After 7 days of culture, the impact of composite hydrogels on the angiogenic differentiation of PDLSCs was assessed. The results showed that the addition of composite hydrogel significantly boosted the expression of the angiogenic gene (VEGF), which was prominent in both the SFD/CS/ZIF-8 and SFD/CS/ZIF-8@QCT groups with no noteworthy difference between them (Fig. 5K). Immunofluorescence staining images confirmed that Pg. LPS did not affect VEGF expression, while the SFD/CS/ZIF-8@QCT group exhibited the highest VEGF protein secretion among the three composite hydrogel groups (Fig. 5L-M). Moreover, our composites exhibit favorable cytocompatibility for human umbilical vein endothelial cells (HUEVCs) (Figure S13, Supporting Information). As shown in Fig. 5N, the control group, the Pg.LPS group and the SFD/CS group induced very limited tube formation, whereas the SFD/CS/ZIF-8 and SFD/CS/ZIF8@QCT induced significantly more tube formation. In addition, quantitative analysis showed that the total length and the number of junctions in the SFD/CS/ZIF8@QCT group were significantly more than that of the SFD/CS/ZIF8 group (Fig. 5O and P). As illustrated in Fig. 5Q–S, the results demonstrated that the incorporation of SFD/CS/ZIF-8 and SFD/CS/ZIF-8@QCT composite hydrogels markedly enhanced the angiogenic gene expression (bFGF, VEGF and vWF) of HUVECs, with the latter exhibiting a more pronounced effect than the former.

Our previous studies have shown that quercetin could speed up the process of angiogenic differentiation of BMSCs in osteoporosis [70]. On the other hand, zinc element has been extensively documented in literatures as having a favorable impact on angiogenesis [71,72]. In conclusion, thanks to the co-secretion of zinc ions and quercetin, the addition of ZIF-8@QCT not only better enhanced the osteogenic induction function of the SFD/CS hydrogel in the inflammatory microenvironment, but also superior promoted the secretion of vascular factors, which could be helpful for vascularized alveolar bone regeneration under periodontitis, compared with the composite hydrogel group with the addition of ZIF-8 (Fig. 5T).

2.7. Effect of composite hydrogels on recruitment of PDLSCs under periodontitis

Areas of bone defects are typically deficient in endogenous MSCs, and the migratory abilities of MSCs in patients with periodontitis are significantly hindered [73]. Thus, on the basis of shaping a pro-osteo-/angiogenic microenvironment, endowing biomaterials with the function of promoting endogenous MSCs recruitment is an added advantage for in situ reconstruction of damaged alveolar bone tissues in the periodontitis microenvironment [74]. In this section, we evaluated the migratory capacity of PDLSCs under the periodontitis microenvironment and the therapeutic efficacy of the composite hydrogels through the transwell assay and scratch test. As depicted in Figures S14A-B (Supporting Information), the quantity of migrated PDLSCs was notably lower in the Pg.LPS group compared to the control group, while the group treated with composite hydrogels showed a significant increase in the number of migrated PDLSCs compared to the Pg. LPS group, with the pro-migration effect increasing in the following grouping order: SFD/CS, SFD/CS/ZIF-8, and SFD/CS/ZIF-8@QCT. With the exception of the migration area of the SFD/CS group, which showed no significant difference from that of the Pg. LPS group, the scratch test results displayed a mostly consistent trend with the migration experiments (Figure S15A-B, Supporting Information). Previous studies had indicated that zinc ions could expedite cell migration by activating zinc-dependent histone deacetylases (HDAC), while quercetin could enhance cell migration by augmenting surface αV integrin and reducing β1 integrin [75,76]. These theoretical mechanisms could potentially explain our observation that SFD/CS/ZIF-8@QCT could efficiently reverse the inhibition of cell migration caused by Pg. LPS (Figure S16, Supporting Information).

2.8. Therapeutic effects of composite hydrogels on alveolar bone defects under periodontitis in vivo

Based on the exceptional therapeutic properties of SFD/CS/ZIF-8@QCT exhibited in the *in vitro* experimental group described above, we proceeded to apply it to a rat alveolar bone defect model with periodontitis in order to assess its therapeutic potential *in vivo* (Fig. 6A). Initially, 3D micro-computed tomography (micro-CT) reconstruction and bone volume/total volume (BV/TV) analysis showed a significant enhancement of bone defect regeneration in periodontitis microenvironment with the addition of composite hydrogels. Except for the first week, during which the regeneration effect was not significant due to the short period of time, SFD/CS/ZIF-8@QCT group exhibited the most potent restorative effect in the 4 and 8 weeks, followed by SFD/CS/ZIF-8 group, and lastly SFD/CS group (Fig. 6B–C).

To further analyze the new bone formation, validation of decalcified bone specimens was performed using Masson trichrome staining (Fig. 6D). It was found that samples treated with SFD/CS/ZIF-8@QCT significantly promoted bone regeneration when compared with other groups. The thickness and width of defects were almost completely reconstructed. These findings were consistent with the 3D reconstruction results. Furthermore, analysis of the Masson staining results also exhibited that a small quantity of hydrogel remained in the bone defect area without completely new bone formation, which suggested that the degradation rate of our biomaterials matched the bone formation rate.

Immunohistofluorescence staining was further performed to investigate the immunomodulatory and osteo-/angiogenic functions of composite hydrogels (Fig. 6E–K). We detected the highest expression of iNOS and the lowest expression of CD206 in the blank group in our study. Double staining images of M1 marker iNOS or M2 marker CD206 together with the macrophage's marker F4/80 displayed a remarkably higher iNOS-positive level and a significantly lower CD206-positive level in Blank and SFD/CS groups than SFD/CS/ZIF-8 and SFD/CS/ZIF-8@QCT groups, while SFD/CS/ZIF-8@QCT group showed the lowest iNOS but highest CD206 expression among all groups (Fig. 6E–F) [77]. Quantitative data of the ratios of iNOS or CD206 macrophages also showed the same tendency with a decreased trend of the iNOS/F4/80 macrophages but an increased change of the CD206/F4/80 macrophages in Blank, SFD/CS, SFD/CS/ZIF-8, and SFD/CS/ZIF-8@QCT groups, confirming that M2 macrophages were successfully and largely induced by the SFD/CS/ZIF-8@QCT hydrogel (Fig. 6G–H). The group treated with SFD/CS/ZIF-8@QCT demonstrated superior immunomodulatory effects, possibly owing to the concurrent discharge of quercetin and zinc ions. Moreover, there were changes in osteogenic (OPN) and angiogenic (CD31) marker expression, but there was no significant difference in facilitation between the SFD/CS/ZIF-8 and SFD/CS/ZIF-8@QCT groups (Fig. 6I–K). Taken together, the above *in vivo* findings suggested that SFD/CS/ZIF-8@QCT effectively facilitated alveolar bone regeneration in the periodontitis microenvironment, while mitigating local inflammation and remodeling the immune microenvironment. This could potentially offer a new avenue for

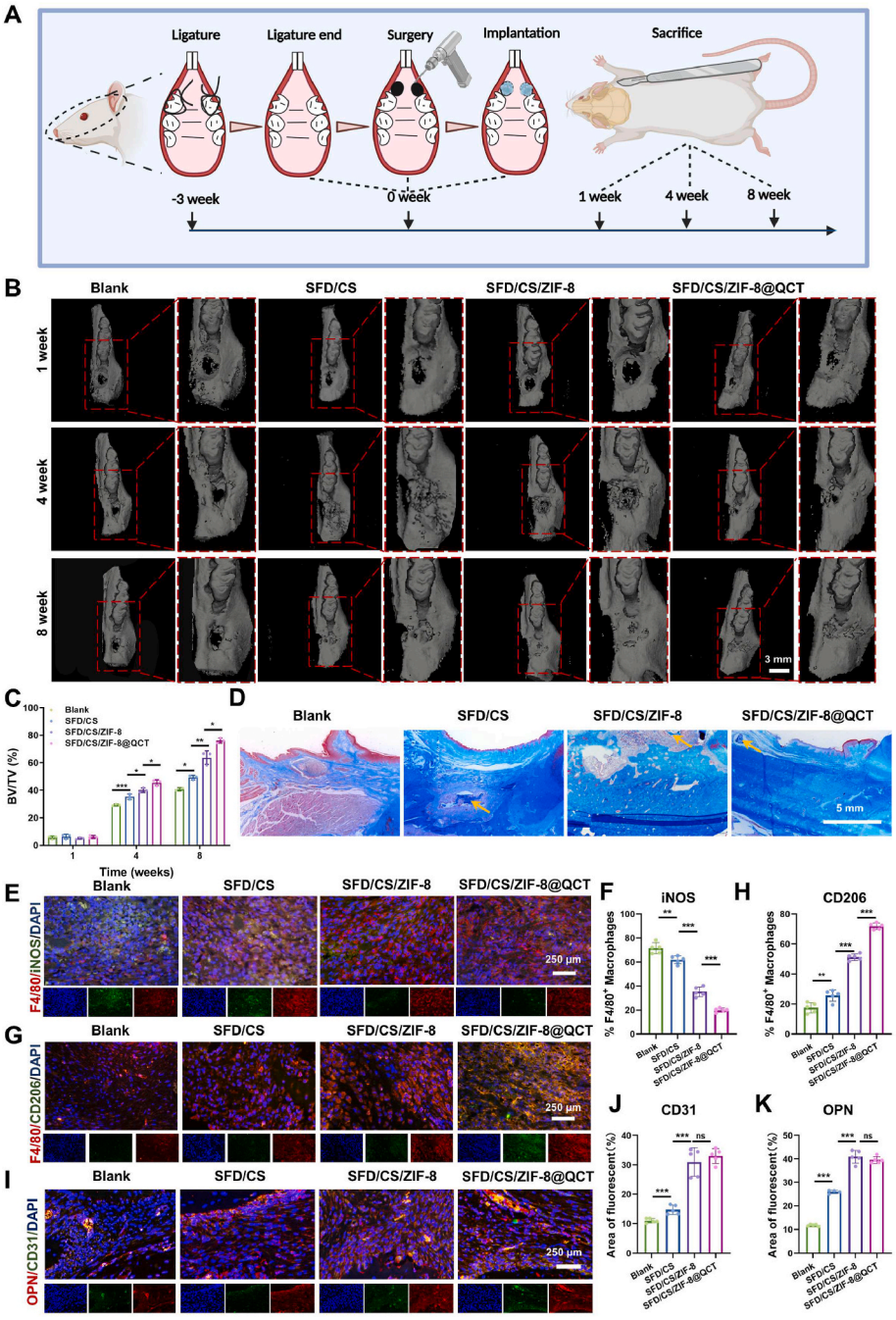

Fig. 6. Therapeutic effects of composite hydrogels on alveolar bone defects under periodontitis *in vivo*. A) Schematic illustration depicting the animal model establishment and the experimental process. B) 3D reconstructed images from micro-CT scanning of rat alveolar bone defects implanted with different composite hydrogels. C) Quantitative analysis of the BV/TV (%) as determined by micro-CT. D) Masson-trichrome staining images (Yellow arrows pointed to nondegraded biomaterials). E-H) The immunofluorescence staining and its quantitative analysis of M1-related marker (iNOS), M2-related marker (CD206) and pan-macrophage marker (F4/80). I–K) The immunofluorescence staining and its quantitative analysis of angiogenesis-related marker (VEGF) and osteogenesis-related marker (OPN). Data are presented as mean ± SD. *P < 0.05, **P < 0.01, and ***P < 0.001; ns, not significant.

treating alveolar bone defects in periodontitis.

2.9. The cellular mechanisms of PDLSCs osteo-/angiogenesis treated by composite hydrogels

To examine the cellular mechanisms through which SFD/CS/ZIF-8@QCT restored osteo-/angiogenic differentiation of PDLSCs during periodontitis, we carried out RNA-Seq. Principal component analysis (PCA) showed that SFD/CS, SFD/CS/ZIF-8 and SFD/CS/ZIF-8@QCT all caused a significant change in the transcriptome of PDLSCs under the periodontitis microenvironment, with these changes being considerably more pronounced than those observed between the Control group and the Pg.LPS group (Figure S17A, Supporting Information). The results demonstrated that 29 and 4 genes exhibited increased and decreased expression, respectively, in the Pg. LPS group in comparison to the control group, while a pronounced change was observed in the treatment of SFD/CS, SFD/CS/ZIF-8 and SFD/CS/ZIF-8@QCT in comparison to the Pg. LPS group (SFD/CS: 2541 down-regulated genes and 2651 up-regulated genes; SFD/CS/ZIF-8: 991 down-regulated genes and 1527 up-regulated genes; SFD/CS/ZIF-8@QCT:1429 down-regulated genes and

913 up-regulated genes) (Figure S17B-E, Supporting Information). The differential expressed genes (DEGs) involved among five groups in the study were grouped into 15 clusters using the hclust function in the R package (Fig. 7A). Among them, significantly upregulated genes after hydrogel treatment were mainly found in cluster 3, 4, 6, 7, 8, 10, 13 and 14, whose enrichment analyses were then analyzed by Metascape. The Gene oncology (GO) and Kyoto Encyclopedia of Genes and Genomes (KEGG) enrichment analysis were performed on the genes within the above clusters, primarily focusing on metabolic, immune system and locomotion processes, with particular emphasis on glycolysis/gluconeogenesis and oxidative phosphorylation (OXPHOS) among metabolic processes. Besides, the PI3K-Akt and HIF-α signaling pathways were also enriched in these clusters (Figure S18A-H and Figure S19A-H, Supporting Information). Additionally, further analysis via GO and KEGG between the Pg. LPS and Pg. LPS + SFD/CS/ZIF-8@QCT groups demonstrated again that the enriched biological processes (BP) mainly focused on metabolic (glycolysis/gluconeogenesis and OXPHOS) and immune-related processes, as well as the enriched signaling pathways highlighted PI3K-Akt and HIF-α, while the influence of Pg.LPS also concentrated on these enrichments compared to the control group (Fig. 7B–C; Figure S20 and Figure S21A-C, Supporting Information). Moreover, the results of GO and KEGG analysis between the Pg. LPS and

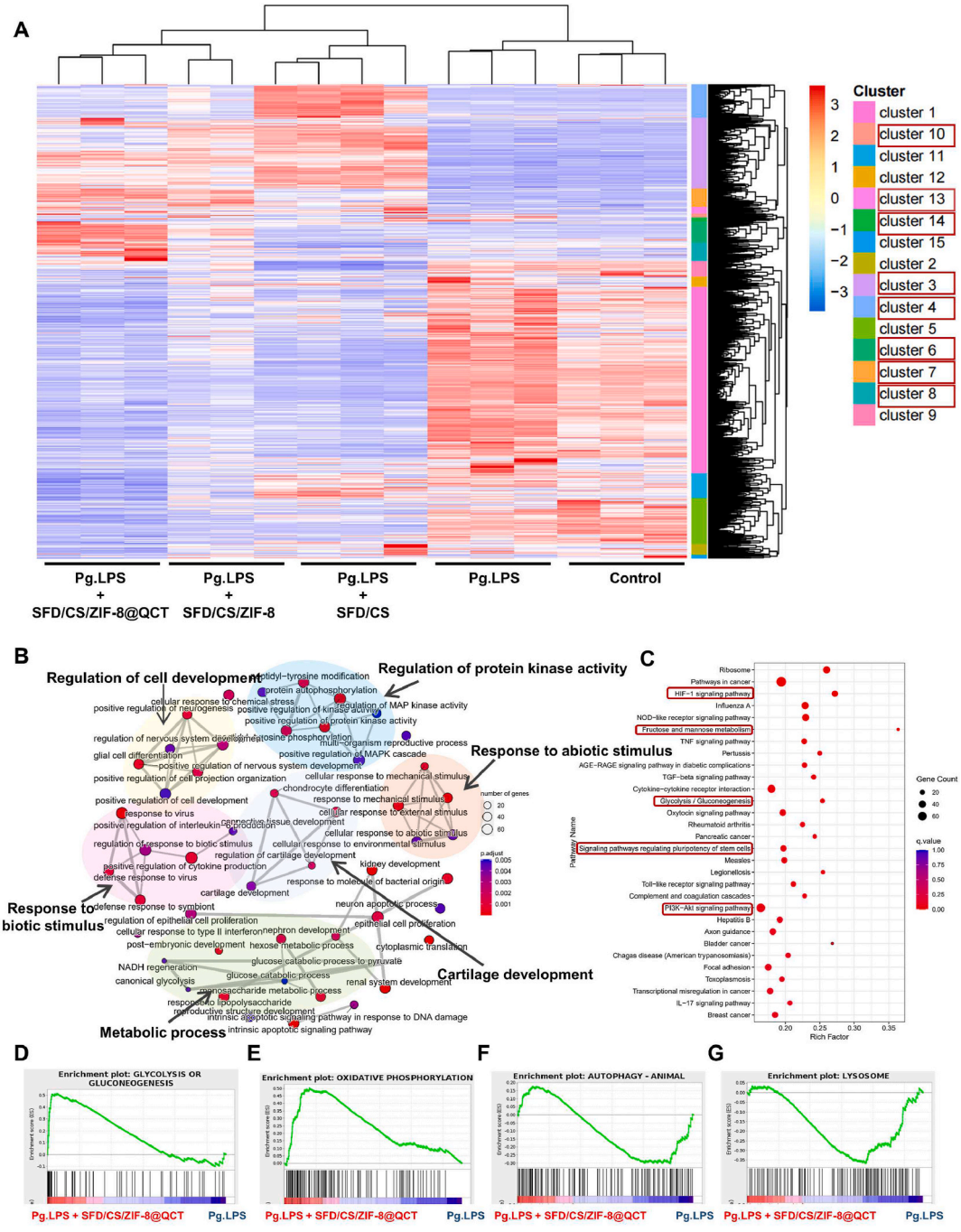

Fig. 7. Cellar mechanism based on RNA-seq and analysis. A) The heat map of DEGs between PDLSCs among Control, Pg.LPS, Pg.LPS + SFD/CS, Pg.LPS + SFD/CS/ZIF-8 and Pg.LPS + SFD/CS/ZIF-8@QCT groups. B, C) The GO enriched network and the KEGG enriched terms of genes between the Pg.LPS and Pg.LPS + SFD/CS/ZIF-8@QCT groups. D-G) GSEA plots of glycolysis/gluconeogenesis, OXPHOS, autophagy and lysosome between the Pg.LPS and Pg.LPS + SFD/CS/ZIF-8@QCT groups.

Pg. LPS + SFD/CS groups as well as the Pg. LPS and Pg. LPS + SFD/CS/ZIF-8 groups were also enriched in the above BP and pathways (Figure S22 A-C and Figure S23A-C, Supporting Information). Subsequently, gene set enrichment analysis (GSEA) revealed that treatment with SFD/CS/ZIF-8@QCT leaded to a significant increase in glycolysis and its downstream OXPHOS process that was previously down-regulated by Pg. LPS treatment, whose inner mechanism might be the enhancement of the translation from D-glucose-6P to phosphoenol-pyruvate as well as the activation of complex I (NADH dehydrogenase), complex III (cytochrome oxidase), and complex V (V-type ATPase) (Fig. 7D–E; Figure S24, Figure S25 and Figure S26 A-B, Supporting Information). Besides, for GSEA result, SFD/CS and SFD/CS/ZIF-8 treatment showed the same trend with the SFD/CS/ZIF-8@QCT treatment (Figure S27A-B and Figure S28A-B, Supporting Information).

Glycolysis and OXPHOS are major cellular metabolic pathways that generate energy and play a key role in biosynthesis and biomineralization. Efficient energy metabolism is crucial for promoting bone regeneration at sites of bone defects [78]. The most essential energy carrier in living organisms is adenosine triphosphate (ATP), which serves as a versatile and convenient currency for energy storage to fuel a diverse range of biochemical reactions within the cell. By examining cellular ATP levels, it was discovered that ATP levels were indeed significantly

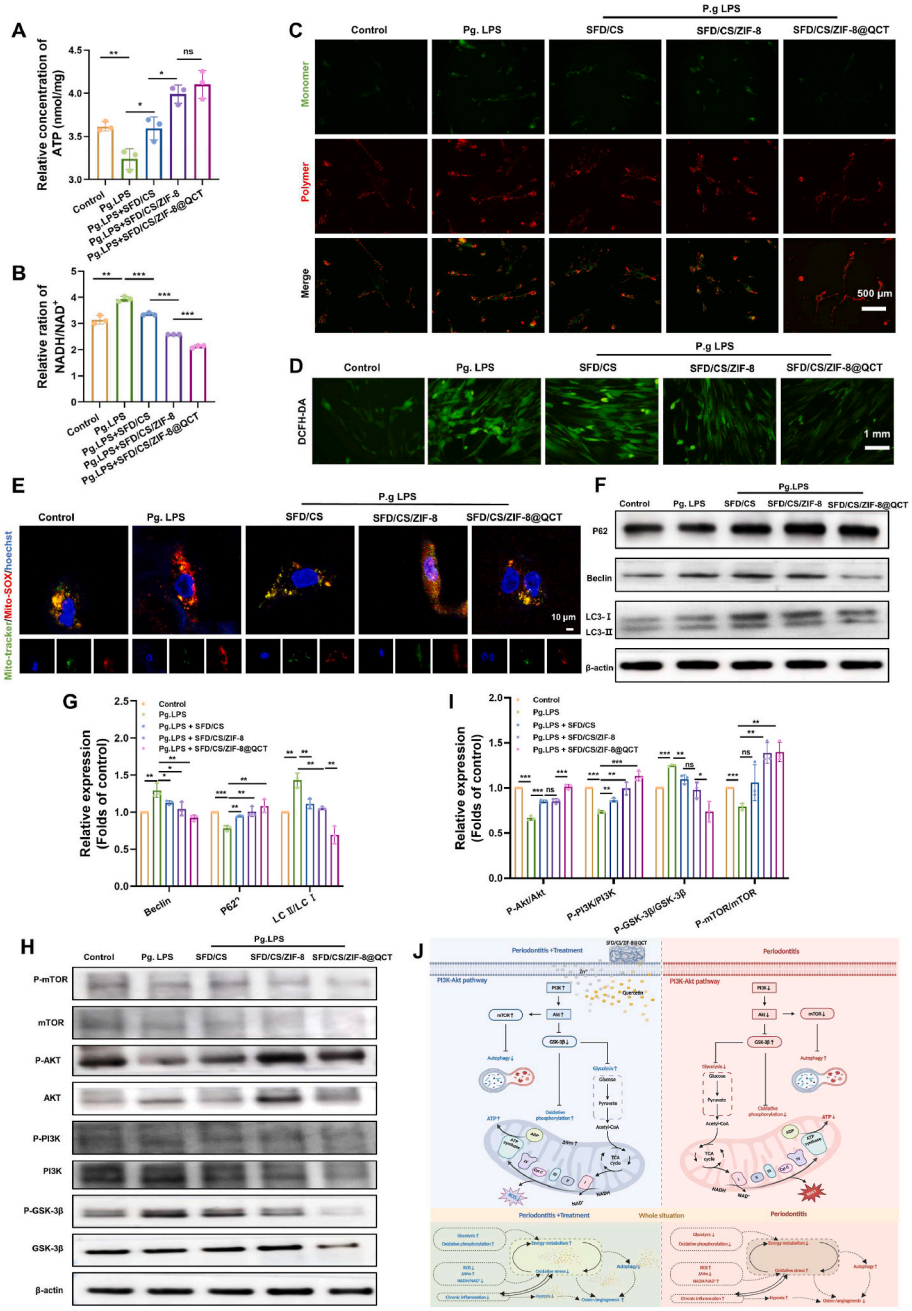

Fig. 8. Verification of RNA-seq results. A, B) The cellular ATP levels and relative NADH/NAD^+ ratios in PDLSCs after different treatments for 7 days, respectively. C) Representative fluorescence images of activated (red) and abnormal (green) mitochondrial membrane potential by JC-1 assay. D, E) Representative fluorescence images of the intracellular and mitochondria ROS level. F–I) Western bolt assay and its quantitative analysis of autophagy-related protein (P62, Beclin and LC3) and PI3K-Akt pathway-related protein (PI3K, Akt, mTOR, GSK-3β) in the PDLSCs after different treatments for 7 days. J) Schematic illustration depicting the therapeutic mechanism of SFD/CS/ZIF-8@QCT on PDLSCs under periodontitis microenvironment. Data are presented as mean ± SD. *P < 0.05, **P < 0.01, and ***P < 0.001; ns, not significant.

reduced in cells in the Pg. LPS group, while the addition of composite hydrogels could increase the ATP production. Among them, SFD/CS/ZIF-8@QCT had the strongest effect on enhancing cellular ATP levels, which may contribute to the improvement of energy metabolism, consistent with the RNA-seq results (Fig. 8A). The aforementioned data indicated that involvement of SFD/CS/ZIF-8@QCT might hasten osteo-/angiogenic differentiation of PDLSCs by activating energy metabolism process that were hindered by Pg. LPS.

Mitochondria, as vital organelles in energy metabolism, play a significant role in maintaining cellular redox homeostasis simultaneously [79]. It has long been recognized that disordered energy metabolism can lead to oxidative stress, which in turn can exacerbate the disturbances in energy metabolism, and this reciprocal cycle can continue and worsen over time [80]. In addition, excessive accumulation of reactive oxygen species (ROS) resulting from oxidative stress exacerbates the inflammatory response in periodontitis, forming a vicious cycle that inhibits alveolar bone regeneration [81].Therefore, harmonizing cellular and mitochondrial redox homeostasis is crucial for repairing alveolar bone defects in the periodontitis microenvironment, in addition to managing energy metabolism and inflammatory response. As shown in Fig. 8B–E, the Pg. LPS group displayed a typical cellular and mitochondrial oxidative stress state, exhibiting an elevation in the NADH/NAD^+ ratio, an increase in the number of JC-1 monomers, as well as an intense rise in both cellular and mitochondrial ROS expression. The addition of SFD/CS/ZIF-8@QCT and SFD/CS/ZIF-8 could obviously reverse the adverse effects of Pg.LPS, with the former exhibiting greater potency than the latter. To date, a substantial amount of research literature confirmed the undeniable antioxidant effects of zinc ions and quercetin [82,83]. Additionally, the catechol group in SFD has been reported to possess the antioxidant effect, but this group experiences facile oxidation and thereby leaded to a significant reduction in its antioxidant effect, which could explain the present but weak antioxidant effect of SFD/CS that we observed in samples co-cultivated with the composite hydrogel for 7 days. The findings indicated that SFD/CS/ZIF-8@QCT could alleviate cellular and mitochondrial oxidative stress in periodontitis, while interrupting the poor energy metabolism—oxidative stress cycle and the hyperinflammatory response—oxidative stress cycle, resulting in beneficial effects on alveolar bone regeneration.

Additionally, the process of autophagy, which is integral to managing cellular equilibrium, was also found to be emphasized in the GSEA, elevated in the Pg. LPS group, and restored in SFD/CS/ZIF-8@QCT group (Fig. 7F–G; Figure S26C-D, Supporting Information). Besides, SFD/CS and SFD/CS/ZIF-8 treatment showed the same trend with the SFD/CS/ZIF-8@QCT treatment (Figure S27C-D and Figure S28C-D, Supporting Information). Autophagy, a pivotal component in preserving cellular homeostasis, can play a significant role in bone regeneration, not just by interacting with energy metabolism, but also by governing molecular degradation and organelle renewal [84]. It has been shown that energy deprivation decreased the ATP level and elevates ROS levels, which leads to the formation of the Mec1-Atg13 complex and activate the energy sensor AMPK-related signaling pathway and thus initiates energy deprivation-induced autophagy [85]. Furthermore, studies also have shown that oxidative stress can trigger autophagy in both cells and mitochondria [86]. Appropriate activation of autophagy contributes to compensating for local energy deficiency and clearing damaged organelles, but excessive and sustained activation leads to apoptosis and worsens tissue damage [87]. Patients with periodontitis exhibit higher autophagy levels in the periodontal membrane and gingival tissues than healthy individuals, while injecting autophagy inhibitors (3-methyladenine or chloroquine) into rats with experimental periodontitis effectively reduced local inflammation and bone resorption [88,89]. Thus, inhibition of over-activated autophagy in the periodontitis microenvironment might contribute to inflammation control and alveolar bone regeneration. Western blot experiments confirmed autophagy activation in PDLSCs after 7 days of culture in a chronic inflammatory microenvironment, which may be partly attributed to impaired energy metabolism and oxidative stress. And the addition of our composite hydrogels all could inhibit the autophagy at the cellular and mitochondrial levels. Among them, the SFD/CS/ZIF-8@QCT hydrogel performed most effective among the three groups, which might be mainly attributed to the direct pharmacological effect of quercetin and the successful interruption of the undesirable energy metabolism-oxidative stress cycle (Fig. 8F-G; Figure S29, Supporting Information) [90].

Based on studies of BP, inspired by the KEGG results, we further evaluate the PI3K-Akt and the HIF-1α signal pathways by Western blot. Our results confirmed that the PI3K-Akt signaling pathway, which plays a vital role in coordinating energy metabolism and autophagy, was suppressed in the periodontitis microenvironment. The application of hydrogels triggered its activation, whose influence on its downstream turned out to be the activation of mammalian target of rapamycin (mTOR) expression (the inhibitor of autophagy) and the inhibition of glycogen synthase kinase-3β (GSK-3β) expression (the activator of glycolysis and OXPHOS) (Fig. 8H–I). Of all the hydrogel groups tested, the SFD/CS/ZIF-8 group exhibited the highest level of activation of the PI3K-AKT signaling pathway. It has been well documented that activation of the PI3K-Akt signaling pathway contributes to the differentiation of MSCs in the osteogenic direction [91]. mTOR is a key protein kinase that regulates autophagy, and its activation inhibits autophagy [92]. GSK-3β is a multifunctional kinase that regulates glycogen metabolism, and its activation inhibits glycolysis by suppressing the expression of glycolysis -associated proteins, such as glucose transporter protein-1 (GLUT-1), GLUT-3, and pyruvate kinase isoform M2 (PKM2) [93]. In addition, GSK-3β inactivation has been reported to activate the OXPHOS through enhancing the expression of OXPHOS complex sub-units [94]. To sum up, we can draw the following conclusions: (i) SFD/CS/ZIF-8@QCT can potentially boost energy metabolism by activating the PI3K/Akt/GSK-3β pathway, which in turn inhibits oxidative stress as well as disrupts the harmful cycle of poor energy metabolism and oxidative stress in the periodontitis microenvironment. (ii) The inhibited PI3K/Akt/mTOR pathway synergizes the vicious cycle of poor energy metabolism and oxidative stress resulting in over-activated autophagy under periodontitis, whereas the addition of SFD/CS/ZIF-8@QCT can significantly reverse the above pathological signaling pathways and biological processes.

On the other hand, it has been reported in the literature that the chronic inflammatory microenvironment of periodontitis creates a localized hypoxic microenvironment, which leads to the activation of the HIF-1α signaling pathway, and the activated HIF-1α signaling pathway inhibits osteogenic differentiation of PDLSCs [95]. The increase expression of HIF-1α in Pg.LPS group was consistent with previous results, while the HIF-1α signaling pathway was negatively regulated by SFD/CS/ZIF-8@QCT (Figure S30, Supporting Information).

Taken together, disturbed energy metabolism and oxidative stress are causative and mutually reinforcing in the periodontitis microenvironment. And the malignant effect of both of them may become the cause of localized hypoxic microenvironment formation and autophagy over-activation, further worsening the disease progression. Attributed to the synergistic effects of quercetin and zinc ions, SFD/CS/ZIF-8@QCT can promote osteo-/angiogenic differentiation of PDLSCs in the periodontitis microenvironment by activating energy metabolism, remodeling redox homeostasis, inhibiting over-activated autophagy and improving hypoxic microenvironment, possibly through activation of the PI3K-Akt signaling pathway (Fig. 8J).

Although our results have demonstrated the superior efficacy of SFD/CS/ZIF-8@QCT in promoting alveolar bone regeneration under the periodontitis microenvironment, it is important to note that the study still has some limitations. It is crucial to acknowledge that periodontitis is a complex disease that affects not only the bone tissue but also the surrounding soft tissues (gingiva and periodontal ligament). Consequently, further research is required to achieve complete periodontal

support tissue regeneration (integration of bone and soft tissues) based on the findings of this study.

3. Conclusion

In summary, the composite hydrogel that we prepared exhibits good thermo-sensitive and adhesive properties. Unlike many current hydrogels which focus on only one or two stages of antibacterial, anti-inflammatory, and healing, our composite hydrogel not only comprehensively considers all of the above stages, but also took into account the disadvantages of periodontal surgery (which is prone to bleeding) and the lack of endogenous MSCs in the periodontal defect area, succeeding in realizing the five-in-one approach. In this study, we observed the outstanding therapeutic effectiveness of SFD/CS/ZIF-8@QCT in advancing the regeneration of alveolar bone defects caused in periodontitis. Furthermore, we clarified the mechanism through which SFD/CS/ZIF-8@QCT re-established the local bone regenerative properties by organizing energy metabolism, oxidative stress, and autophagy. Our findings suggest that the SFD/CS/ZIF-8@QCT hydrogel is effective in promoting *in vivo* and *in vitro* alveolar bone regeneration in periodontitis, demonstrating significant potential for application in periodontitis treatment.

Ethics approval and consent to participate

The animal study was approved by the Independent Ethics Committee of Shanghai Ninth People's Hospital affiliated with Shanghai JiaoTong University, School of Medicine (SH9H-2020-A469-1). The PDLSCs extracted from human teeth approved by the Clinical Ethics Committee of the Ninth People's Hospital of Shanghai Jiao Tong University (SH9H-2022-T370-1).

Data availability statement

The data that support the findings of this study are available from the corresponding author upon reasonable request.

CRediT authorship contribution statement

Shiyuan Yang: Writing – original draft, Software, Methodology, Investigation, Formal analysis. **Yan Zhu:** Methodology, Formal analysis. **Chunxiao Ji:** Methodology, Formal analysis. **Huimin Zhu:** Methodology. **An Lao:** Methodology. **Ran Zhao:** Methodology. **Yue Hu:** Methodology. **Yuning Zhou:** Methodology. **Jia Zhou:** Methodology. **Kaili Lin:** Writing – review & editing, Project administration, Methodology, Data curation, Conceptualization. **Yuanjin Xu:** Writing – review & editing, Supervision, Resources, Project administration, Conceptualization.

Declaration of competing interest

The authors declare no conflict of interest.

Acknowledgements

This work was supported by National Natural Science Foundation of China (82370921, 82071082), Program of Shanghai Technology Research Leader (23XD1430800), Fund of Department of Oral and Maxillofacial Surgery (Department 2023-01). The authors would like to thank Biorender software (https://www.biorender.com/) for its picture source assistance during the preparation of this manuscript.

Appendix A. Supplementary data

Supplementary data to this article can be found online at https://doi.org/10.1016/j.bioactmat.2024.07.016.

References

[1] J. Slots, Periodontitis: facts, fallacies and the future, Periodontol. 2000 75 (1) (2017) 7–23, https://doi.org/10.1111/prd.12221.
[2] D.F. Kinane, P.G. Stathopoulou, P.N. Papapanou, Periodontal diseases, Nat. Rev. Dis. Prim. 3 (2017) 17038, https://doi.org/10.1038/nrdp.2017.38.
[3] J. Luan, R. Li, W. Xu, H. Sun, Q. Li, D. Wang, S. Dong, J. Ding, Functional biomaterials for comprehensive periodontitis therapy, Acta Pharm. Sin. B 13 (6) (2023) 2310–2333, https://doi.org/10.1016/j.apsb.2022.10.026.
[4] N. Li, L. Xie, Y. Wu, Y. Wu, Y. Liu, Y. Gao, J. Yang, X. Zhang, L. Jiang, Dexamethasone-loaded zeolitic imidazolate frameworks nanocomposite hydrogel with antibacterial and anti-inflammatory effects for periodontitis treatment, Mater Today Bio 16 (2022) 100360, https://doi.org/10.1016/j.mtbio.2022.100360.
[5] A. Javadkhani, B. Shokouhi, A. Mosayebzadeh, S. Safa, M. Fahimi, S. Sharifi, S. Maleki Dizaj, S. Salatin, Nano-catechin gel as a sustained release antimicrobial agent against clinically isolated porphyromonas gingivalis for promising treatment of periodontal diseases, Biomedicines 11 (7) (2023) 1932, https://doi.org/10.3390/biomedicines11071932.
[6] S. Hu, L. Wang, J. Li, D. Li, H. Zeng, T. Chen, L. Li, X. Xiang, Catechol-modified and MnO(2)-nanozyme-reinforced hydrogel with improved antioxidant and antibacterial capacity for periodontitis treatment, ACS Biomater. Sci. Eng. 9 (9) (2023) 5332–5346, https://doi.org/10.1021/acsbiomaterials.3c00454.
[7] S. Liu, Y.-n. Wang, B. Ma, J. Shao, H. Liu, S. Ge, Gingipain-responsive thermosensitive hydrogel loaded with SDF-1 facilitates in situ periodontal tissue regeneration, ACS Appl. Mater. Interfaces 13 (31) (2021) 36880–36893, https://doi.org/10.1021/acsami.1c08855.
[8] J. Gong, C. Ye, J. Ran, X. Xiong, X. Fang, X. Zhou, Y. Yi, X. Lu, J. Wang, C. Xie, J. Liu, Polydopamine-Mediated immunomodulatory patch for diabetic periodontal tissue regeneration assisted by metformin-ZIF system, ACS Nano 17 (17) (2023) 16573–16586, https://doi.org/10.1021/acsnano.3c02407.
[9] M. Locati, G. Curtale, A. Mantovani, Diversity, mechanisms, and significance of macrophage plasticity, Annu. Rev. Pathol. 15 (2020) 123–147, https://doi.org/10.1146/annurev-pathmechdis-012418-012718.
[10] X. Sun, J. Gao, X. Meng, X. Lu, L. Zhang, R. Chen, Polarized macrophages in periodontitis: characteristics, function, and molecular signaling, Front. Immunol. 12 (2021) 763334, https://doi.org/10.3389/fimmu.2021.763334.
[11] Y. Cui, S. Hong, Y. Xia, X. Li, X. He, X. Hu, Y. Li, X. Wang, K. Lin, L. Mao, Melatonin engineering M2 macrophage-derived exosomes mediate endoplasmic reticulum stress and immune reprogramming for periodontitis therapy, Adv. Sci. 10 (27) (2023) e2302029, https://doi.org/10.1002/advs.202302029.
[12] G. Liu, L. Zhang, X. Zhou, J. Xue, R. Xia, X. Gan, C. Lv, Y. Zhang, X. Mao, X. Kou, S. Shi, Z. Chen, Inducing the "re-development state" of periodontal ligament cells via tuning macrophage mediated immune microenvironment, J. Adv. Res. 60 (2024) 233–248, https://doi.org/10.1016/j.jare.2023.08.009.
[13] L. Lin, S. Li, S. Hu, W. Yu, B. Jiang, C. Mao, G. Li, R. Yang, X. Miao, M. Jin, Y. Gu, E. Lu, UCHL1 impairs periodontal ligament stem cell osteogenesis in periodontitis, J. Dent. Res. 102 (1) (2023) 61–71, https://doi.org/10.1177/00220345221116031.
[14] J. Yu, S. Chen, S. Lei, F. Li, Y. Wang, X. Shu, W. Xu, X. Tang, The effects of porphyromonas gingivalis on inflammatory and immune responses and osteogenesis of mesenchymal stem cells, Stem Cell. Dev. 30 (24) (2021) 1191–1201, https://doi.org/10.1089/scd.2021.0068.
[15] M. Wu, H. Liu, D. Li, Y. Zhu, P. Wu, Z. Chen, F. Chen, Y. Chen, Z. Deng, L. Cai, Smart-responsive multifunctional therapeutic system for improved regenerative microenvironment and accelerated bone regeneration via mild photothermal therapy 11 (2) (2024) 2304641, https://doi.org/10.1002/advs.202304641.
[16] J.L. Mark Welch, S.T. Ramírez-Puebla, G.G. Borisy, Oral microbiome geography: micron-scale habitat and niche, Cell Host Microbe 28 (2) (2020) 160–168, https://doi.org/10.1016/j.chom.2020.07.009.
[17] S. Xu, B. Hu, T. Dong, B.Y. Chen, X.J. Xiong, L.J. Du, Y.L. Li, Y.L. Chen, G.C. Tian, X.B. Bai, T. Liu, L.J. Zhou, W.C. Zhang, Y. Liu, Q.F. Ding, X.Q. Zhang, S.Z. Duan, Alleviate periodontitis and its comorbidity hypertension using a nanoparticle-embedded functional hydrogel system, Adv. Healthcare Mater. 12 (20) (2023) e2203337, https://doi.org/10.1002/adhm.202203337.
[18] C. Zong, W. Van Holm, A. Bronckaers, Z. Zhao, S. Čokić, M.K. Aktan, A.B. Castro, B. Van Meerbeek, A. Braem, G. Willems, M. Cadenas de Llano-Pérula, Biomimetic periodontal ligament transplantation activated by gold nanoparticles protects alveolar bone, Adv. Healthcare Mater. 12 (15) (2023) e2300328, https://doi.org/10.1002/adhm.202300328.
[19] S. Ren, Y. Zhou, K. Zheng, X. Xu, J. Yang, X. Wang, L. Miao, H. Wei, Y. Xu, Cerium oxide nanoparticles loaded nanofibrous membranes promote bone regeneration for periodontal tissue engineering, Bioact. Mater. 7 (2022) 242–253, https://doi.org/10.1016/j.bioactmat.2021.05.037.
[20] D.K. Khajuria, O.N. Patil, D. Karasik, R. Razdan, Development and evaluation of novel biodegradable chitosan based metformin intrapocket dental film for the management of periodontitis and alveolar bone loss in a rat model, Arch. Oral Biol. 85 (2018) 120–129, https://doi.org/10.1016/j.archoralbio.2017.10.009.
[21] D.K. Khajuria, S.F. Zahra, R. Razdan, Effect of locally administered novel biodegradable chitosan based risedronate/zinc-hydroxyapatite intra-pocket dental film on alveolar bone density in rat model of periodontitis, J. Biomater. Sci. Polym. Ed. 29 (1) (2018) 74–91, https://doi.org/10.1080/09205063.2017.1400145.
[22] X. Xu, Z. Gu, X. Chen, C. Shi, C. Liu, M. Liu, L. Wang, M. Sun, K. Zhang, Q. Liu, Y. Shen, C. Lin, B. Yang, H. Sun, An injectable and thermosensitive hydrogel: promoting periodontal regeneration by controlled-release of aspirin and erythropoietin, Acta Biomater. 86 (2019) 235–246, https://doi.org/10.1016/j.actbio.2019.01.001.

[23] Y. Liu, T. Li, M. Sun, Z. Cheng, W. Jia, K. Jiao, S. Wang, K. Jiang, Y. Yang, Z. Dai, L. Liu, G. Liu, Y. Luo, ZIF-8 modified multifunctional injectable photopolymerizable GelMA hydrogel for the treatment of periodontitis, Acta Biomater. 146 (2022) 37–48, https://doi.org/10.1016/j.actbio.2022.03.046.
[24] X. Zhang, Z. Wang, H. Jiang, H. Zeng, N. An, B. Liu, L. Sun, Z. Fan, Self-powered enzyme-linked microneedle patch for scar-prevention healing of diabetic wounds, Sci. Adv. 9 (28) (2023) eadh1415, https://doi.org/10.1126/sciadv.adh1415.
[25] I. Sahibdad, S. Khalid, G.R. Chaudhry, A. Salim, S. Begum, I. Khan, Zinc enhances the cell adhesion, migration, and self-renewal potential of human umbilical cord derived mesenchymal stem cells, World J. Stem Cell. 15 (7) (2023) 751–767, https://doi.org/10.4252/wjsc.v15.i7.751.
[26] A. Lao, J. Wu, D. Li, A. Shen, Y. Li, Y. Zhuang, K. Lin, J. Wu, J. Liu, Functionalized metal-organic framework-modified hydrogel that breaks the vicious cycle of inflammation and ROS for repairing of diabetic bone defects, Small 19 (36) (2023) e2206919, https://doi.org/10.1002/smll.202206919.
[27] Y. Wang, C. Li, Y. Wan, M. Qi, Q. Chen, Y. Sun, X. Sun, J. Fang, L. Fu, L. Xu, B. Dong, L. Wang, Quercetin-loaded ceria nanocomposite potentiate dual-directional immunoregulation via macrophage polarization against periodontal inflammation, Small 17 (41) (2021) e2101505, https://doi.org/10.1002/smll.202101505.
[28] W. Zhang, L. Jia, B. Zhao, Y. Xiong, Y.N. Wang, J. Liang, X. Xu, Quercetin reverses TNF-α induced osteogenic damage to human periodontal ligament stem cells by suppressing the NF-κB/NLRP3 inflammasome pathway, Int. J. Mol. Med. 47 (4) (2021) 39, https://doi.org/10.3892/ijmm.2021.4872.
[29] Z. He, X. Zhang, Z. Song, L. Li, H. Chang, S. Li, W. Zhou, Quercetin inhibits virulence properties of Porphyromas gingivalis in periodontal disease, Sci. Rep. 10 (1) (2020) 18313, https://doi.org/10.1038/s41598-020-74977-y.
[30] F. Irfan, F. Jameel, I. Khan, R. Aslam, S. Faizi, A. Salim, Role of quercetin and rutin in enhancing the therapeutic potential of mesenchymal stem cells for cold induced burn wound, Regen Ther 21 (2022) 225–238, https://doi.org/10.1016/j.reth.2022.07.011.
[31] F. Jia, S. Lin, X. He, J. Zhang, S. Shen, Z. Wang, B. Tang, C. Li, Y. Wu, L. Dong, K. Cheng, W. Weng, Comprehensive evaluation of surface potential characteristics on mesenchymal stem cells' osteogenic differentiation, ACS Appl. Mater. Interfaces 11 (25) (2019) 22218–22227, https://doi.org/10.1021/acsami.9b07161.
[32] S.M. Pustulka, K. Ling, S.L. Pish, J.A. Champion, Protein nanoparticle charge and hydrophobicity govern protein corona and macrophage uptake, ACS Appl. Mater. Interfaces 12 (43) (2020) 48284–48295, https://doi.org/10.1021/acsami.0c12341.
[33] B. Xiao, Y. Liu, I. Chandrasiri, C. Overby, D.S.W. Benoit, Impact of nanoparticle physicochemical properties on protein corona and macrophage polarization, ACS Appl. Mater. Interfaces 15 (11) (2023) 13993–14004, https://doi.org/10.1021/acsami.2c22471.
[34] Y. Wang, T. Ying, J. Li, Y. Xu, R. Wang, Q. Ke, S.G.F. Shen, H. Xu, K. Lin, Hierarchical micro/nanofibrous scaffolds incorporated with curcumin and zinc ion eutectic metal organic frameworks for enhanced diabetic wound healing via anti-oxidant and anti-inflammatory activities, Chem. Eng. J. 402 (2020) 126273, https://doi.org/10.1016/j.cej.2020.126273.
[35] M.-P. Tian, A.-D. Zhang, Y.-X. Yao, X.-G. Chen, Y. Liu, Mussel-inspired adhesive and polypeptide-based antibacterial thermo-sensitive hydroxybutyl chitosan hydrogel as BMSCs 3D culture matrix for wound healing, Carbohydr. Polym. 261 (2021) 117878, https://doi.org/10.1016/j.carbpol.2021.117878.
[36] R. Ahmed, N. ul ain Hira, M. Wang, S. Iqbal, J. Yi, Y. Hemar, Genipin, a natural blue colorant precursor: source, extraction, properties, and applications, Food Chem. 434 (2024) 137498, https://doi.org/10.1016/j.foodchem.2023.137498.
[37] L. Lu, S. Yuan, J. Wang, Y. Shen, S. Deng, L. Xie, Q. Yang, The Formation mechanism of hydrogels, Curr. Stem Cell Res. Ther. 13 (7) (2018) 490–496, https://doi.org/10.2174/1574888x12666170612102706.
[38] K. Zhang, K. Xue, X.J. Loh, Thermo-responsive hydrogels: from recent progress to biomedical applications, Gels 7 (3) (2021) 77, https://doi.org/10.3390/gels7030077.
[39] S. Azevedo, A.M.S. Costa, A. Andersen, I.S. Choi, H. Birkedal, J.F. Mano, Bioinspired ultratough hydrogel with fast recovery, self-healing, injectability and cytocompatibility, Adv. Mater. 29 (28) (2017), https://doi.org/10.1002/adma.201700759, 10.1002/adma.201700759.
[40] X. Lin, H. Zhang, S. Li, L. Huang, R. Zhang, L. Zhang, A. Yu, B. Duan, Polyphenol-driving assembly for constructing chitin-polyphenol-metal hydrogel as wound dressing, Carbohydr. Polym. 290 (2022) 119444, https://doi.org/10.1016/j.carbpol.2022.119444.
[41] Y. Zhang, X. Dou, L. Zhang, H. Wang, T. Zhang, R. Bai, Q. Sun, X. Wang, T. Yu, D. Wu, B. Han, X. Deng, Facile fabrication of a biocompatible composite gel with sustained release of aspirin for bone regeneration, Bioact. Mater. 11 (2022) 130–139, https://doi.org/10.1016/j.bioactmat.2021.09.033.
[42] C. Shen, M.M. Wang, L. Witek, N. Tovar, B.N. Cronstein, A. Torroni, R.L. Flores, P. G. Coelho, Transforming the degradation rate of β-tricalcium phosphate bone replacement using 3-dimensional printing, Ann. Plast. Surg. 87 (6) (2021) e153–e162, https://doi.org/10.1097/sap.0000000000002965.
[43] Y. Peng, Q.J. Liu, T. He, K. Ye, X. Yao, J. Ding, Degradation rate affords a dynamic cue to regulate stem cells beyond varied matrix stiffness, Biomaterials 178 (2018) 467–480, https://doi.org/10.1016/j.biomaterials.2018.04.021.
[44] W. Zhang, R. Wang, Z. Sun, X. Zhu, Q. Zhao, T. Zhang, A. Cholewinski, F.K. Yang, B. Zhao, R. Pinnaratip, P.K. Forooshani, B.P. Lee, Catechol-functionalized hydrogels: biomimetic design, adhesion mechanism, and biomedical applications, Chem. Soc. Rev. 49 (2) (2020) 433–464, https://doi.org/10.1039/c9cs00285e.
[45] S. Choi, J.R. Moon, N. Park, J. Im, Y.E. Kim, J.H. Kim, J. Kim, Bone-adhesive anisotropic tough hydrogel mimicking tendon enthesis, Adv. Mater. 35 (3) (2023) e2206207, https://doi.org/10.1002/adma.202206207.
[46] W. Cai, J. Wang, C. Chu, W. Chen, C. Wu, G. Liu, Metal-organic framework-based stimuli-responsive systems for drug delivery, Adv. Sci. 6 (1) (2019) 1801526, https://doi.org/10.1002/advs.201801526.
[47] L. Jia, N. Han, J. Du, L. Guo, Z. Luo, Y. Liu, Pathogenesis of important virulence factors of porphyromonas gingivalis via toll-like receptors, Front. Cell. Infect. Microbiol. 9 (2019) 262, https://doi.org/10.3389/fcimb.2019.00262.
[48] C. Ardean, C.M. Davidescu, N.S. Nemeş, A. Negrea, M. Ciopec, N. Duteanu, P. Negrea, D. Duda-Seiman, V. Musta, Factors influencing the antibacterial activity of chitosan and chitosan modified by functionalization, Int. J. Mol. Sci. 22 (14) (2021) 7449, https://doi.org/10.3390/ijms22147449.
[49] S. Yao, J. Chi, Y. Wang, Y. Zhao, Y. Luo, Y. Wang, Zn-MOF encapsulated antibacterial and degradable microneedles array for promoting wound healing, Adv. Healthcare Mater. 10 (12) (2021) e2100056, https://doi.org/10.1002/adhm.202100056.
[50] T. Kwon, I.B. Lamster, L. Levin, Current concepts in the management of periodontitis, Int. Dent. J. 71 (6) (2021) 462–476, https://doi.org/10.1111/idj.12630.
[51] Y. Zheng, K. Shariati, M. Ghovvati, S. Vo, N. Origer, T. Imahori, N. Kaneko, N. Annabi, Hemostatic patch with ultra-strengthened mechanical properties for efficient adhesion to wet surfaces, Biomaterials 301 (2023) 122240, https://doi.org/10.1016/j.biomaterials.2023.122240.
[52] X. Lu, Z. Liu, Q. Jia, Q. Wang, Q. Zhang, X. Li, J. Yu, B. Ding, Flexible bioactive glass nanofiber-based self-expanding cryogels with superelasticity and bioadhesion enabling hemostasis and wound healing, ACS Nano 17 (12) (2023) 11507–11520, https://doi.org/10.1021/acsnano.3c01370.
[53] M. Shin, S.G. Park, B.C. Oh, K. Kim, S. Jo, M.S. Lee, S.S. Oh, S.H. Hong, E.C. Shin, K.S. Kim, S.W. Kang, H. Lee, Complete prevention of blood loss with self-sealing haemostatic needles, Nat. Mater. 16 (1) (2017) 147–152, https://doi.org/10.1038/nmat4758.
[54] Y. Du, X. Chen, L. Li, H. Zheng, A. Yang, H. Li, G. Lv, Benzeneboronic–alginate/quaternized chitosan–catechol powder with rapid self-gelation, wet adhesion, biodegradation and antibacterial activity for non-compressible hemorrhage control, Carbohydr. Polym. 318 (2023) 121049, https://doi.org/10.1016/j.carbpol.2023.121049.
[55] M. Pan, Z. Tang, J. Tu, Z. Wang, Q. Chen, R. Xiao, H. Liu, Porous chitosan microspheres containing zinc ion for enhanced thrombosis and hemostasis, Mater. Sci. Eng. C 85 (2018) 27–36, https://doi.org/10.1016/j.msec.2017.12.015.
[56] J. Lin, D. Huang, H. Xu, F. Zhan, X. Tan, Macrophages: a communication network linking Porphyromonas gingivalis infection and associated systemic diseases, Front. Immunol. 13 (2022) 952040, https://doi.org/10.3389/fimmu.2022.952040.
[57] Y. Xiong, Z. Lin, P. Bu, T. Yu, Y. Endo, W. Zhou, Y. Sun, F. Cao, G. Dai, Y. Hu, L. Lu, L. Chen, P. Cheng, K. Zha, M.-A. Shahbazi, Q. Feng, B. Mi, G. Liu, A whole-course-repair system based on neurogenesis-angiogenesis crosstalk and macrophage reprogramming promotes diabetic wound healing, Adv. Mater. 35 (19) (2023) 2212300, https://doi.org/10.1002/adma.202212300.
[58] X. Bai, D. Chen, Y. Dai, S. Liang, B. Song, J. Guo, B. Dai, D. Zhang, L. Feng, Bone formation recovery with gold nanoparticle-induced M2 macrophage polarization in mice, Nanomedicine 38 (2021) 102457, https://doi.org/10.1016/j.nano.2021.102457.
[59] B. Xiao, Y. Liu, I. Chandrasiri, E. Adjei-Sowah, J. Mereness, M. Yan, D.S.W. Benoit, Bone-targeted nanoparticle drug delivery system-mediated macrophage modulation for enhanced fracture healing 20 (7) (2024) 2305336, https://doi.org/10.1002/smll.202305336.
[60] C. Ding, C. Yang, T. Cheng, X. Wang, Q. Wang, R. He, S. Sang, K. Zhu, D. Xu, J. Wang, X. Liu, X. Zhang, Macrophage-biomimetic porous Se@SiO(2) nanocomposites for dual modal immunotherapy against inflammatory osteolysis, J. Nanobiotechnol. 19 (1) (2021) 382, https://doi.org/10.1186/s12951-021-01128-4.
[61] W. Zhou, Z. Lin, Y. Xiong, H. Xue, W. Song, T. Yu, L. Chen, Y. Hu, A.C. Panayi, Y. Sun, F. Cao, G. Liu, L. Hu, C. Yan, X. Xie, W. Qiu, B. Mi, G. Liu, Dual-targeted nanoplatform regulating the bone immune microenvironment enhances fracture healing, ACS Appl. Mater. Interfaces 13 (48) (2021) 56944–56960, https://doi.org/10.1021/acsami.1c17420.
[62] K. Liu, X. Dong, Y. Wang, X. Wu, H. Dai, Dopamine-modified chitosan hydrogel for spinal cord injury, Carbohydr. Polym. 298 (2022) 120047, https://doi.org/10.1016/j.carbpol.2022.120047.
[63] M. Jarosz, M. Olbert, G. Wyszogrodzka, K. Młyniec, T. Librowski, Antioxidant and anti-inflammatory effects of zinc. Zinc-dependent NF-κB signaling, Inflammopharmacology 25 (1) (2017) 11–24, https://doi.org/10.1007/s10787-017-0309-4.
[64] C.F. Tsai, G.W. Chen, Y.C. Chen, C.K. Shen, D.Y. Lu, L.Y. Yang, J.H. Chen, W.L. Yeh, Regulatory effects of quercetin on M1/M2 macrophage polarization and oxidative/antioxidative balance, Nutrients 14 (1) (2021) 67, https://doi.org/10.3390/nu14010067.
[65] A. Tomokiyo, N. Wada, H. Maeda, Periodontal ligament stem cells: regenerative potency in periodontium, Stem Cell. Dev. 28 (15) (2019) 974–985, https://doi.org/10.1089/scd.2019.0031.
[66] Z. Chen, W. Zhang, M. Wang, L.J. Backman, J. Chen, Effects of zinc, magnesium, and iron ions on bone tissue engineering, ACS Biomater. Sci. Eng. 8 (6) (2022) 2321–2335, https://doi.org/10.1021/acsbiomaterials.2c00368.
[67] A.D. Inchingolo, A.M. Inchingolo, G. Malcangi, P. Avantario, D. Azzollini, S. Buongiorno, F. Viapiano, M. Campanelli, A.M. Ciocia, N. De Leonardis, E. de

Ruvo, I. Ferrara, G. Garofoli, V. Montenegro, A. Netti, G. Palmieri, A. Mancini, A. Patano, F. Piras, G. Marinelli, C. Di Pede, C. Laudadio, B. Rapone, D. Hazballa, A. Corriero, M.C. Fatone, A. Palermo, F. Lorusso, A. Scarano, I.R. Bordea, D. Di Venere, F. Inchingolo, G. Dipalma, Effects of resveratrol, curcumin and quercetin supplementation on bone metabolism-A systematic review, Nutrients 14 (17) (2022) 3519, https://doi.org/10.3390/nu14173519.

[68] A. Merkel, Y. Chen, C. Villani, A. George, GRP78 promotes the osteogenic and angiogenic response in periodontal ligament stem cells, Eur. Cell. Mater. 45 (2023) 14–30, https://doi.org/10.22203/eCM.v045a02.

[69] F. Zhao, Z. Yang, H. Xiong, Y. Yan, X. Chen, L. Shao, A bioactive glass functional hydrogel enhances bone augmentation via synergistic angiogenesis, self-swelling and osteogenesis, Bioact. Mater. 22 (2023) 201–210, https://doi.org/10.1016/j.bioactmat.2022.09.007.

[70] Y. Zhou, Y. Wu, W. Ma, X. Jiang, A. Takemra, M. Uemura, L. Xia, K. Lin, Y. Xu, The effect of quercetin delivery system on osteogenesis and angiogenesis under osteoporotic conditions, J. Mater. Chem. B 5 (3) (2017) 612–625, https://doi.org/10.1039/c6tb02312f.

[71] W.Q. Zhu, K. Li, S. Su, W. Chen, Y. Liu, J. Qiu, Effects of zinc ions released from Ti-nw-Zn surface on osteogenesis and angiogenesis in vitro and in an in vivo zebrafish model, Front. Bioeng. Biotechnol. 10 (2022) 848769, https://doi.org/10.3389/fbioe.2022.848769.

[72] L. Yu, Y. Yin, Z. Guo, Y. Fei, X. Wen, J. Wang, H. Sun, J. Hu, S. Jin, A functional study of zinc-titanium coatings and exploration of the intrinsic correlation between angiogenesis and osteogenesis, J. Mater. Chem. B 11 (14) (2023) 3236–3251, https://doi.org/10.1039/d3tb00119a.

[73] P. Wang, H. Tian, Z. Zhang, Z. Wang, EZH2 regulates lipopolysaccharide-induced periodontal ligament stem cell proliferation and osteogenesis through TLR4/MyD88/NF-κB pathway, Stem Cell. Int. 2021 (2021) 7625134, https://doi.org/10.1155/2021/7625134.

[74] H. Wang, X. Chang, Q. Ma, B. Sun, H. Li, J. Zhou, Y. Hu, X. Yang, J. Li, X. Chen, J. Song, Bioinspired drug-delivery system emulating the natural bone healing cascade for diabetic periodontal bone regeneration, Bioact. Mater. 21 (2023) 324–339, https://doi.org/10.1016/j.bioactmat.2022.08.029.

[75] S.T. Huang, R.C. Yang, H.T. Wu, C.N. Wang, J.H. Pang, Zinc-chelation contributes to the anti-angiogenic effect of ellagic acid on inhibiting MMP-2 activity, cell migration and tube formation, PLoS One 6 (5) (2011) e18986, https://doi.org/10.1371/journal.pone.0018986.

[76] C. Chittasupho, A. Manthaisong, S. Okonogi, S. Tadtong, W. Samee, Effects of quercetin and curcumin combination on antibacterial, antioxidant, in vitro wound healing and migration of human dermal fibroblast cells, Int. J. Mol. Sci. 23 (1) (2021) 142, https://doi.org/10.3390/ijms23010142.

[77] Z. Tu, M. Chen, M. Wang, Z. Shao, X. Jiang, K. Wang, Z. Yao, S. Yang, X. Zhang, W. Gao, C. Lin, B. Lei, C. Mao, Engineering bioactive M2 macrophage-polarized anti-inflammatory, antioxidant, and antibacterial scaffolds for rapid angiogenesis and diabetic wound repair 31 (30) (2021) 2100924, https://doi.org/10.1002/adfm.202100924.

[78] S. Lin, S. Yin, J. Shi, G. Yang, X. Wen, W. Zhang, M. Zhou, X. Jiang, Orchestration of energy metabolism and osteogenesis by Mg(2+) facilitates low-dose BMP-2-driven regeneration, Bioact. Mater. 18 (2022) 116–127, https://doi.org/10.1016/j.bioactmat.2022.03.024.

[79] H.M. Rabah, D.A. Mohamed, R.A. Mariah, S.R. Abd El-Khalik, H.A. Khattab, N. A. AbuoHashish, A.M. Abdelsattar, M.A. Raslan, E.E. Farghal, A.K. Eltokhy, Novel insights into the synergistic effects of selenium nanoparticles and metformin treatment of letrozole-induced polycystic ovarian syndrome: targeting PI3K/Akt signalling pathway, redox status and mitochondrial dysfunction in ovarian tissue, Redox Rep. 28 (1) (2023) 2160569, https://doi.org/10.1080/13510002.2022.2160569.

[80] C. Quijano, M. Trujillo, L. Castro, A. Trostchansky, Interplay between oxidant species and energy metabolism, Redox Biol. 8 (2016) 28–42, https://doi.org/10.1016/j.redox.2015.11.010.

[81] X. Qiu, Y. Yu, H. Liu, X. Li, W. Sun, W. Wu, C. Liu, L. Miao, Remodeling the periodontitis microenvironment for osteogenesis by using a reactive oxygen species-cleavable nanoplatform, Acta Biomater. 135 (2021) 593–605, https://doi.org/10.1016/j.actbio.2021.08.009.

[82] C. Hübner, H. Haase, Interactions of zinc- and redox-signaling pathways, Redox Biol. 41 (2021) 101916, https://doi.org/10.1016/j.redox.2021.101916.

[83] D. Xu, M.J. Hu, Y.Q. Wang, Y.L. Cui, Antioxidant activities of quercetin and its complexes for medicinal application, Molecules 24 (6) (2019) 1123, https://doi.org/10.3390/molecules24061123.

[84] J. Wang, Y. Zhang, J. Cao, Y. Wang, N. Anwar, Z. Zhang, D. Zhang, Y. Ma, Y. Xiao, L. Xiao, X. Wang, The role of autophagy in bone metabolism and clinical significance, Autophagy 19 (9) (2023) 2409–2427, https://doi.org/10.1080/15548627.2023.2186112.

[85] W. Yao, Y. Li, Y. Chen, Y. Chen, P. Zhao, Y. Zhang, Q. Jiang, Y. Feng, F. Yang, C. Wu, H. Zhong, Y. Zhou, Q. Sun, L. Zhang, W. Liu, C. Yi, Mec1 regulates PAS recruitment of Atg13 via direct binding with Atg13 during glucose starvation-induced autophagy, Proc. Natl. Acad. Sci. U. S. A. 120 (1) (2023) e2215126120, https://doi.org/10.1073/pnas.2215126120.

[86] C. Garza-Lombó, A. Pappa, M.I. Panayiotidis, R. Franco, Redox homeostasis, oxidative stress and mitophagy, Mitochondrion 51 (2020) 105–117, https://doi.org/10.1016/j.mito.2020.01.002.

[87] A.C. Racanelli, S.A. Kikkers, A.M.K. Choi, S.M. Cloonan, Autophagy and inflammation in chronic respiratory disease, Autophagy 14 (2) (2018) 221–232, https://doi.org/10.1080/15548627.2017.1389823.

[88] W.J. Kim, S.Y. Park, O.S. Kim, H.S. Park, J.Y. Jung, Autophagy upregulates inflammatory cytokines in gingival tissue of patients with periodontitis and lipopolysaccharide-stimulated human gingival fibroblasts, J. Periodontol. 93 (3) (2022) 380–391, https://doi.org/10.1002/jper.21-0178.

[89] S. He, Q. Zhou, B. Luo, B. Chen, L. Li, F. Yan, Chloroquine and 3-methyladenine attenuates periodontal inflammation and bone loss in experimental periodontitis, Inflammation 43 (1) (2020) 220–230, https://doi.org/10.1007/s10753-019-01111-0.

[90] L. Wu, Q. Zhang, W. Mo, J. Feng, S. Li, J. Li, T. Liu, S. Xu, W. Wang, X. Lu, Q. Yu, K. Chen, Y. Xia, J. Lu, L. Xu, Y. Zhou, X. Fan, C. Guo, Quercetin prevents hepatic fibrosis by inhibiting hepatic stellate cell activation and reducing autophagy via the TGF-β1/Smads and PI3K/Akt pathways, Sci. Rep. 7 (1) (2017) 9289, https://doi.org/10.1038/s41598-017-09673-5.

[91] J. Long, Z. Yao, W. Zhang, B. Liu, K. Chen, L. Li, B. Teng, X.F. Du, C. Li, X.F. Yu, L. Qin, Y. Lai, Regulation of osteoimmune microenvironment and osteogenesis by 3D-printed PLAG/black phosphorus scaffolds for bone regeneration, Adv. Sci. (2023) e2302539, https://doi.org/10.1002/advs.202302539.

[92] L. Ma, R. Zhang, D. Li, T. Qiao, X. Guo, Fluoride regulates chondrocyte proliferation and autophagy via PI3K/AKT/mTOR signaling pathway, Chem. Biol. Interact. 349 (2021) 109659, https://doi.org/10.1016/j.cbi.2021.109659.

[93] H. Huang, J. Xue, T. Xie, M.L. Xie, Osthole increases the radiosensitivity of hepatoma cells by inhibiting GSK-3β/AMPK/mTOR pathway-controlled glycolysis, Naunyn-Schmiedeberg's Arch. Pharmacol. 396 (4) (2023) 683–692, https://doi.org/10.1007/s00210-022-02347-8.

[94] W.F. Theeuwes, H.R. Gosker, R.C.J. Langen, N.A.M. Pansters, A. Schols, A.H. V. Remels, Inactivation of glycogen synthase kinase 3β (GSK-3β) enhances mitochondrial biogenesis during myogenesis, Biochim. Biophys. Acta, Mol. Basis Dis. 1864 (9 Pt B) (2018) 2913–2926, https://doi.org/10.1016/j.bbadis.2018.06.002.

[95] Z. Liu, L. Guo, R. Li, Q. Xu, J. Yang, J. Chen, M. Deng, Transforming growth factor-β1 and hypoxia inducible factor-1α synergistically inhibit the osteogenesis of periodontal ligament stem cells, Int. Immunopharm. 75 (2019) 105834, https://doi.org/10.1016/j.intimp.2019.105834.